frontiers in Oncology

REVIEW
published: 22 December 2017
doi: 10.3389/fonc.2017.00314

Fluorescence-Guided Surgery

*Tadanobu Nagaya, Yu A. Nakamura, Peter L. Choyke and Hisataka Kobayashi**

Molecular Imaging Program, Center for Cancer Research, National Cancer Institute, National Institutes of Health, Bethesda, MD, United States

Surgical resection of cancer remains an important treatment modality. Despite advances in preoperative imaging, surgery itself is primarily guided by the surgeon's ability to locate pathology with conventional white light imaging. Fluorescence-guided surgery (FGS) can be used to define tumor location and margins during the procedure. Intraoperative visualization of tumors may not only allow more complete resections but also improve safety by avoiding unnecessary damage to normal tissue which can also reduce operative time and decrease the need for second-look surgeries. A number of new FGS imaging probes have recently been developed, complementing a small but useful number of existing probes. In this review, we describe current and new fluorescent probes that may assist FGS.

OPEN ACCESS

Edited by:
Marie-France Penet, Johns Hopkins University, United States

Reviewed by:
Luigi Aloj, Cambridge University Hospitals NHS Foundation Trust, United Kingdom
Laurence Gluch, The Strathfield Breast Centre, Australia

***Correspondence:**
Hisataka Kobayashi
kobayash@mail.nih.gov

Specialty section:
This article was submitted to Cancer Imaging and Diagnosis, a section of the journal Frontiers in Oncology

Received: *27 October 2017*
Accepted: *05 December 2017*
Published: *22 December 2017*

Citation:
Nagaya T, Nakamura YA, Choyke PL and Kobayashi H (2017) Fluorescence-Guided Surgery. Front. Oncol. 7:314. doi: 10.3389/fonc.2017.00314

Keywords: fluorescence-guided surgery, activatable probe, monoclonal antibodies, molecular imaging, always-on probe

INTRODUCTION

Surgery is a primary mode of treatment for many malignancies. For example, 63–98% of patients with lung, breast, bladder, and colorectal cancer will undergo surgery (1). The goal of surgery is to safely remove as much cancer as possible. The degree to which cancer is removed relates closely to prognosis. However, the ability to resect tumor currently relies on the visual localization of the tumor and/or the ability to palpate it. The former is limited by the low contrast between tumors and background tissue and many small tumors may be missed. Moreover, the determination of tumor margins must often be done blindly followed by frozen section pathologic analysis.

The presence of residual tumor cells after resection is considered a strong predictor of tumor recurrence and, therefore, survival. Many studies show that positive margins, defined as the identification of tumor cells at the cut edge of a surgical specimen, are associated with increased local recurrence and indicate a poor prognosis in most cancer types including head and neck cancers (2), breast cancer (3, 4), non-small-cell lung cancer (5), colorectal cancer (6), bladder cancer (7), and prostate cancer (8). Despite advances in preoperative imaging such as computerized tomography (CT), magnetic resonance imaging (MRI), and positron emission tomography, surgical margin positivity rate has not changed significantly over the past several decades (9), with margin positivity rates of 15–60% across all cancers (10–16). Currently, the standard of care for achieving negative

Abbreviations: AAA, abdominal aortic aneurysm; ALA, aminolevulinic acid; ADC, antibody-drug-conjugate; APC, antibody-photo-absorber conjugate; CA, carbohydrate antigen; CABG, coronary artery bypass grafting; CEA, carcinoembryonic antigen; CT, computerized tomography; epidermal growth factor receptor; FDA, Food and Drug Administration; FGS, fluorescence-guided surgery; FITC, fluorescein isothiocyanate; FLARE, fluorescence-assisted resection and exploration; FRET, Föster (fluorescence) resonance energy transfer; gGlu, γ-glutamyl; GGT, γ-glutamyltransferase; H-dimer, homo-dimers; HLA, hexaminolevulinate; HMRG, hydroxymethyl rhodamine green; ICG, indocyanine green; mAb, monoclonal antibodies; MB, methylene blue; MMP, matrix metalloproteinase; MRI, magnetic resonance imaging; NDA, New Drug Application, NIR, near-infrared; PET, positron emission tomography; PeT, photon induced electron transfer; PIT, photoimmunotherapy; Pp, protoporphyrin; PSMA, prostate-specific membrane antigen; SLN, sentinel lymph node; TBR, target-to-background ratio; VEGF, vascular endothelial growth factor.

margins rests on visual inspection, palpation, and intraoperative histopathological analysis of frozen tumor margins all of which have severe limitations. The naked eye is limited in its ability to detect small tumors. Palpation is limited in sensitivity and is increasingly not used due to the increased utilization of robotic laparoscopic surgery. Intraoperative frozen section analysis is limited to certain tissue types, is time-consuming, and is prone to sampling error. Frozen section analysis is discrepant with permanent pathology in 5–15% of cases (17).

A number of non-optical imaging methods have been proposed during surgery. Typically, these methods are not targeted to the tumor *per se* but rely on anatomic abnormalities to define the tumor. For instance, intraoperative CT and MRI have played a significant role in the field of neurosurgical image guidance (18–20). However, intraoperative systems are costly, complex and require space. Moreover, their use interrupts the normal workflow of the surgical procedure lengthening operative/anesthesia times. These methods are, mainly used for neurosurgery at major medical centers.

Therefore, practical methods for augmenting the surgeon's ability to resect tumors are needed. One such method is fluorescence-guided surgery (FGS). The first use of fluorescence imaging in surgery dates back to 1948 when surgeons used intravenous fluorescein to enhance intracranial neoplasms during neurosurgery (21). Since then, additional fluorescent agents have been used for a variety of surgical applications (22–24). Intraoperative fluorescence imaging offers the benefits of high contrast and sensitivity, low cost, absence of ionizing radiation, ease of use, safety, and high specificity (25, 26). Compared with standard unaided vision using white light imaging, real-time fluorescence imaging is helpful in identifying cancerous tissue and delineating tumor margins. Moreover, improved visualization of the cancer can reduce damage to important normal structures such as nerves, blood vessels, ureters, and bile ducts.

In this review article, we focus on the currently used Food and Drug Administration (FDA)-approved fluorescent probes and new types of fluorescence imaging probes for FGS that are under development.

CURRENT FGS

The exponential growth in the field of FGS is demonstrated by the number of published articles in the field, which has grown from under 50/year in 1995, to nearly 500/year in 2015 (27). Furthermore, FGS has enjoyed a number of preliminary successes (23, 28) and some FGS techniques have already achieved clinical success (29). FGS may improve tumor resection rates while minimizing normal tissue resection (9, 30, 31). This can translate into improved clinical outcomes.

Compared to expensive traditional imaging methods, optical methods are less costly and require less space. One cost estimate of the fluorescence-assisted resection and exploration (FLARE) system is 120,000 USD and 40,000 USD for the mini-FLARE (32, 33). Of course, this does not include the cost of the optical probe itself but the overall costs are much lower than with conventional imaging. Moreover, because it is portable a single instrument could be shared among multiple operating rooms.

Fluorescence-guided surgery has been currently used for multiple surgical situations, including sentinel lymph node (SLN) mapping, identification of solid tumors, lymphography, angiography, and anatomical imaging during surgery. Importantly, FGS can be used seamlessly during the procedure without interrupting the surgeon's workflow. This integrates FGS into the surgery creating numerous opportunities for its use. We summarize current clinical and preclinical FGS techniques in **Table 1**.

TABLE 1 | Current clinical and preclinical fluorescence-guided surgery techniques.

Application	Types	Contrast agent	Status
Sentinel lymph node mapping	Breast cancer	Indocyanine green (ICG) (34–37)	Clinical
		Methylene blue (MB) (38, 39)	Clinical
	Melanoma	ICG (40, 41)	Clinical
	Head and neck cancer	ICG (42)	Clinical
	Lung cancer	ICG (43)	Clinical
	Esophagus cancer	ICG (44, 45)	Clinical
	Gastric cancer	ICG (46, 47)	Clinical
	Colorectal cancer	ICG (48)	Clinical
	Anal cancer	ICG (49)	Clinical
	Prostate cancer	ICG (50–52)	Clinical
	Penile cancer	ICG (51, 52)	Clinical
Lymphography	Lymph flow	ICG (53–55)	Clinical
Angiography	Cerebral aneurysm	Fluorescein sodium (56–58)	Clinical
	Coronary artery bypass grafting	ICG (59, 60)	Clinical
	Abdominal aortic aneurysm	ICG (61)	Clinical
	Abdominal surgery	ICG (62, 63)	Clinical
	Reconstructive surgery	ICG (64–70)	Clinical
Anatomic imaging	Cholangiography	ICG (71, 72)	Clinical
	Pancreas	MB (73)	Preclinical
		T700-F (74)	Preclinical
	Ureters	MB (75)	Preclinical
	Nerves	Various fluorescently labeled peptide (NP) (76, 77)	Preclinical
	Parathyroid and thyroid grands	T700 and T800 fluorophores (78)	Preclinical
	Endocrine grands	Various near-infrared fluorophores (79–81)	Preclinical
Tumor imaging	Malignant glioma	5-ALA (82–86)	Clinical
		Fluorescein sodium (87–89)	Clinical
		BLZ-100 (90)	Clinical
		GB119 (91)	Preclinical
	Brain metastases	Fluorescein sodium (92, 93)	Clinical
	Head and neck cancer	IRDye800CW conjugate (94, 95)	Clinical
		IRDye700DX conjugate (96)	Clinical
	Hepatocellular carcinoma	ICG (97–100)	Clinical
	Liver metastases	ICG (99)	Clinical
	Breast cancer	MB (101)	Clinical
		EC17 (102)	Clinical
		IRDye800CW conjugate (102)	Clinical
		LUM015 (103)	Clinical
		AVB-620 (104)	Clinical

(*Continued*)

TABLE 1 | Continued

Application	Types	Contrast agent	Status
	Lung and chest masses	ICG (105)	Clinical
		Folate-fluorescein isothiocyanate (FITC) (106)	Clinical
		EC17 (107)	Clinical
		OTL38 (108)	Clinical
	Ovarian cancer	ICG (109)	Clinical
		Folate-FITC (28)	Clinical
		EC17 (110)	Clinical
		OTL38 (111)	Clinical
		gGlu-HMRG (112)	Preclinical
	Pancreatic cancer	Green fluorophore conjugate (113, 114)	Preclinical
		IRDye800CW conjugate (102)	Preclinical
	Insulinoma	MB (73)	Preclinical
	Solitary fibrous tumor (pancreas)	MB (115)	Preclinical
	Renal cell carcinoma	EC17 (116)	Clinical
		OTL38 (102)	Clinical
	Bladder cancer	5-ALA/HAL (117–120)	Clinical
	Prostate cancer	ICG conjugate (121)	Preclinical
		5-ALA (122)	Clinical
	Gastric cancer	ICG (123–125)	Clinical
	Colorectal cancer	Green fluorophore conjugate (113)	Preclinical
		IRDye800CW conjugate (126)	Clinical
		gGlu-HMRG (127)	Preclinical
	Basal cell carcinoma	5-ALA (128)	Clinical
		GB119 (129)	Preclinical
	Sarcoma	LUM015 (103)	Clinical
	Parathyroid adenoma	MB (130)	Clinical
Laparoscopic- and robotic-assisted surgeries	Nephrectomy	ICG (131)	Clinical
	Cholecystectomy	ICG (72, 132)	Clinical
	Esophagectomy	ICG (133)	Clinical
	Gastrectomy	ICG (134)	Clinical
	Adrenalectomy	ICG (135, 136)	Clinical
Fluorescence endoscopy	Brain aneurysm	ICG (137–139)	Clinical
	Endonasal surgery	ICG (140–142)	Clinical
	Angiography	ICG (142, 143)	Clinical
	Brain tumor	ICG (140, 144, 145)	Clinical
	Head and Neck tumor	ICG (146)	Clinical
	Gastric cancer	ICG (123–125)	Clinical
Marking tumor	Colonic tattooing	ICG (147–149)	Clinical

CLINICALLY AVAILABLE FLUORESCENCE IMAGING

There has been an explosion of interest in FGS, which has led to a steady demand for new fluorescence imaging devices and probes. Currently, most FGS imaging has been performed with the Novadaq SPY system which was the first to be approved by FDA in 2005; however, several new fluorescence imaging systems have subsequently been approved by the FDA as shown in **Table 2**. These systems are approved for a variety of procedures including imaging blood flow, tissue perfusion, and circulation in free flaps, plastic surgery, and reconstructive surgery. These systems are portable making their positioning within a room completely customizeable to the situation. Hand-held cameras of PDE and Fluobeam, for instance, possess the advantage of being compact and convenient for real-time fluorescence imaging. Other cameras such as Quest Spectrum and VS3 Iridium simultaneously show the white light image and the fluorescent probe image overlay which reduces distractions for the surgeon (150, 151). In the field of breast oncology, the SPY system has been applied to monitor skin perfusion in nipple-sparing mastectomies using ICG as the imaging probe. This method can guide the location of mastectomy incisions and minimize ischemic complications (152).

A successful device should be able to display RGB white light imaging, fluorescence imaging, and overlay imaging. The device should be capable of quantitating the light intensity to the extent possible. Quantitation permits FGS to be used in multicenter trials and allows comparison at different time points in the same patient. Further investigations are needed to establish reliable quantitative analyses of fluorescent imaging.

CURRENT CLINICAL USE OF FLUORESCENCE IMAGING PROBES

Biomedical fluorescence imaging operates in wavelengths in the visible spectrum (400–700 nm), extending into the near infrared (NIR) spectrum (700–900 nm). A large number of commercially available fluorophores are available; however, few are clinically approved. While the majority of fluorescent probes emit light in the visible range, this is probably the least desirable part of the spectrum due to overlap with tissue autofluorescence and high absorbance of light in tissue in the visible spectrum. NIR fluorophores are better suited for *in vivo* imaging. While, wavelengths below 700 nm are strongly absorbed in tissue by

TABLE 2 | Clinically available Food and Drug Administration-approved fluorescence imaging systems.

Imaging system	Company	Excitation wavelength(s) (nm)	Light source	Working distance (cm)	Field of view (cm)	Real-time overlay
SPY	Novadaq Technologies	805	Laser	~30	19 × 14	No
PDE	Hamamatsu Photonics	760	LED	~20	5 × 5 to 10 × 6.7	No
Fluobeam 700 (800)	Fluoptics Minatec	680 (750)	Laser	15 ~ 25	2.2 × 1.5 to 20 × 14	No
Quest Spectrum	Quest Medical Imaging	400–1,000	Laser	5~	2.25 × 2.25 (5 cm distance)	Yes
VS3 Iridium system	VisionSense	805	Laser	~30	19 × 14	Yes

endogenous molecules, such as hemoglobin and myoglobin, wavelengths above 900 nm are limited by water and lipid absorption wavelengths (153–155). Fluorophores emitting light <700 or >900 nm are, therefore, limited in their ability to penetrate tissue (156). The "NIR window" from 700 to 900 nm arises from less absorbance in tissues, allowing for deeper imaging and detection (153, 154). Thus, fluorophores in the NIR range have excellent potential for FGS. Fluorescence imaging using NIR fluorophores enhances cancer surgery navigation and offers higher sensitivity when compared to preoperative imaging, visual inspection, and palpation during surgery (157). Next, we will focus on the currently used fluorescence imaging probes in surgical oncology (**Table 3**).

Indocyanine Green (ICG)

Currently, ICG is one of the most frequently employed NIR fluorophores used for FGS. ICG is a water-soluble, anionic, amphiphilic tricarbocyanine probe with a molecular weight of 776 Da (158, 159), which rapidly binds to plasma proteins in the body. The excitation peak is 780 nm and the emission peak is at 820 nm, which places outside the range of most tissue autofluorescence. ICG was first produced in 1955 by the Kodak Research Laboratories, and in 1959 it was approved by the FDA for retinal angiography. Historically, it has been clinically used to measure cardiac output (160), hepatic function (161), and retinal angiography (162).

Throughout its history, ICG has maintained a high safety index (25, 163, 164), as the number of allergic reactions is very low (1:10,000, as reported by manufacturer) (165). ICG also allows multiple repeated uses due to its short half-life of 150 to 180 s and is cleared exclusively by the liver (166).

Near infrared ICG-guided SNL mapping has been performed in various cancers as shown in **Table 1**. ICG has also been used for lymphography (167), angiography (61, 168), reconstructive surgery (65, 67), cholangiography (71) and tumor imaging (99), and so on. The use of ICG for delineating tumors has been a success. For instance, ICG fluorescence imaging identified 100% of primary hepatocellular carcinomas (HCCs) and in 40% of the cases also identified additional, small (3–6 mm) HCCs that would otherwise have gone undetected (98).

TABLE 3 | Currently used Food and Drug Administration-approved fluorescence probes.

Fluorescence probe	Excitation	Emission	Fluorescence type
Indocyanine green	780 nm	820 nm	Indocyanin green
Methylene blue (MB)	670 nm	690 nm	MB
5-Aminolevulinic acid (5-ALA)	380–440 nm	620 nm (alkaline pH) 634 nm (acid pH)	Porphyrin
Fluorescein sodium	494 nm	512 nm	Fluorescein
Folate	495 nm (folate-FITC)	520 nm (folate-FITC)	Fluorescein isothiocyanate (FITC)
IRDye800CW conjugate	775 nm	796 nm	IRDye800
IRDye700DX conjugate	680 nm	687 nm	IRDye700
Activatable probes	Various	Various	Various

Methylene Blue (MB)

Methylene blue is a heterocyclic aromatic compound with a molecular weight of 320 Da (51). It is a FDA-approved visible (dark blue) contrast agent. When sufficiently diluted, MB acts as a near-infrared fluorescent dye that operates within the NIR optical window with an absorption peak at 670 nm and an emission peak at 690 nm and is naturally excreted through the urine (51). MB was the first entirely synthetic drug used in medicine and was used in the treatment of malaria as early as 1891 by Guttmann and Ehrlich (169). MB continues to be applied and investigated as treatment for a variety of medical applications in the clinical setting, including methemoglobinemias and ifosfamide-induced encephalopathy (170, 171). MB has also been used to identify breast cancer (101) and neuroendocrine tumors (73), and is commonly used for SLN mapping (38, 39), as well as the identification of urologic tumors (51, 52) and tumors in the parathyroid glands (130).

Methylene blue is known to be relatively safe; however, the use of MB can potentially lead to cardiac arrhythmias, coronary vasoconstriction, decreased cardiac output, decreased renal blood flow and mesenteric blood flow, and increased pulmonary vascular pressure (172). Although MB accumulates in most tumors, the amount of accumulation varies with tumor type. Therefore, dye concentration appropriately matched to each tumor type is required (38).

5-Aminolevulinic Acid (5-ALA)

5-ALA is the major substrate for protoporphyrin synthesis, and has been used clinically for tumor detection and tumor treatment (photodynamic therapy; PDT), as a FDA-approved substance. 5-ALA, typically administered in a topical or oral form, induces synthesis and accumulation of the fluorescent molecule protoporphyrin IX (PpIX) in epithelia and neoplastic tissues (83, 85, 86). 5-ALA-induced PpIX exhibits multiple physiochemical states depending on the microenvironment. One of the most important parameters affecting the state of PpIX is pH. In the pH range 3 to 11.5, there are two distinct states: emission peaks at 620 nm in alkaline environments and emission peaks at 634 nm in acidic environments after excitation with visible blue light of 380–440 nm (173, 174).

Cancer specific FGS with 5-ALA has been successfully implemented for resection of malignant gliomas in Europe after studies clearly demonstrated clinical benefits with regards to completeness of tumor removal (65% complete resection with 5-ALA compared to 36% in the white light group) and progression-free survival with its use (83). 5-ALA and derivatives have also been described in bladder cancer (117, 118, 120) and prostate cancer (122).

The use of 5-ALA has been limited by its relatively high costs, and an inconvenient method of administration (it is administered orally some hours before it is to be used). The high risk of skin sensitization within 24 h after the operation (the patient should not be exposed to sunlight or strong artificial light) also presents a challenge to its use (175).

Fluorescein Sodium

Fluorescein sodium is a fluorescent drug that can be used intravenously to improve visualization of brain tumor tissue based

primarily on non-specific vascular leakage. It is also used for retinal angiography (56–58). Fluorescein sodium is a sodium salt and an organic fluorescent dye with peak excitation at 494 nm and peak emission at 512 nm. It has been safely used in humans for many years, predominantly in ophthalmology for retinal angiography, and the cost of fluorescein sodium is relatively low when compared with the cost of 5-ALA (176). Fluorescein sodium is usually visible to the naked eye at high dosages (20 mg/kg body weight), and is observable through the yellow 560 nm filter at lower doses, allowing better tissue discrimination with more natural colors (177, 178).

The use of fluorescein sodium for the identification of intracranial tumors has been known since 1947 (179). As an FGS agent, fluorescein sodium has been commonly used for identifying glioblastoma (88) and metastatic brain tumors (92, 93). It has also been used for intracranial angiography (56–58).

NEW FLUORESCENCE IMAGING PROBES

The ideal fluorescence imaging probe must provide excellent contrast between the tumor or affected lymph node and healthy tissue (180). Therefore, a current challenge is to design fluorescent imaging probes with high selectivity for tumors, high tumor to background ratios, and minimal toxicity (155).

Current clinical studies are based on contrast agents that have already been approved. The most often used fluorophores are blood pool agents (including ICG) that have no inherent specificity for tumor or normal tissues, and thus are not ideal fluorophores for FGS. A number of new agents are currently being investigated, including several dyes from the cyanine family, such as Cy5.5, Cy7, Cy7.5, IR-dyes, nanoparticle formulations, and visible spectrum dyes (181). Most research focuses on increasing the availability of novel, fluorescently labeled agents to identify crucial landmarks, such as tumor margins, lymph nodes, and vital structures of interest to surgeons. A new generation of agents that target-specific antigens have been based on antibodies (113, 182, 183), nanobodies (184), aptamers, and peptides (77). Other approaches make use of enzymes for fluorescence activation (185–189).

In the following sections, we summarize progress made in several specific targeted optical imaging agents for FGS.

Folate-Targeted FGS

The Folate receptor is commonly upregulated on tumor cells and, therefore, is a good candidate for a general-purpose fluorescently labeled, targeted agent. An example is folate fluorescein isothiocyanate (folate-FITC) that excites at a wavelength of 495 nm and emits at 520 nm (190). Folate and these folate analogs are internalized in the cell *via* receptor-mediated endocytosis within 2 h (191). Once inside the endosome, the conjugate remains intact and can, therefore, remain fluorescent after internalization (191, 192). This stability led to the development of a broad variety of folate-targeted conjugates. van Dam et al. used a folate fluorescein isothiocyanate to identify tumor implants in ovarian cancer patients who were undergoing abdominal surgery (28). Lung adenocarcinoma is also known to express high levels of folate receptor α (193, 194). This was exploited by Okusanya et al. who demonstrated that lung adenocarcinomas demonstrated fluorescence in 92% (46/50) of patients with folate-FITC (106). Another folate analog, EC17, was also used for imaging renal cell carcinoma, although only two of four cancers were detected (116). In another study using EC17 for intraoperative detection of ovarian cancer, Tummers et al. showed that the addition of FGS resulted in a16% increase in the resection of malignant tumors when compared to visual inspection and palpation (110). Of course, the clinical significance of this increase is still uncertain. Another folate analog, OTL38, has been used to delineate renal cell carcinoma margins during partial nephrectomy (102), and to identify ovarian cancer (111). Hoogstins et al. also reported that OTL38 accumulated in folate receptor α-positive tumors and metastases in 12 patients with ovarian cancer, enabling the surgeon to resect an additional 29% of malignant lesions that were not identified by inspection and/or palpation (111). Recently, both EC17 and OTL38 were also used for intraoperative lung tumor imaging (107, 108). Like all targeted agents, folate-FITC is restricted to use only in tumors over expressing folate receptor and, by virtue of the visible light emitted by FITC, the agent has a limited depth penetration.

Monoclonal Antibody-Based Fluorescent Probes

Perhaps the most generalizable FGS probes are based on monoclonal antibodies (mAb) conjugated to a fluorescent dye. There are at least two scenarios in which mAb-based fluorescent probes could become clinically useful. One is in fluorescence-guided navigation to aid surgeons in detecting tiny lesions and determining the margin between cancer and normal tissue. Another is in selecting patients whose cancer cells express a sufficient amount of target to enable molecularly targeted therapies such as antibody–drug conjugates or antibody-photo-absorber conjugates.

Promising preclinical examples of targeted fluorescently labeled probes include anti carcinoembryonic antigen in pancreatic cancer and colorectal cancer conjugated to a green fluorophore (113), anti carbohydrate antigen 19-9 in pancreatic cancer conjugated to a green fluorophore (114), epidermal growth factor receptor (EGFR) and EGFR type2 (HER2) in breast cancer (195–197) and prostate-specific membrane antigen (PSMA) in prostate cancer conjugated to ICG (121). Most mAb-based fluorescent probes are designed for systemic administration. Compared to other routes of administration, such as oral or intra-tumoral injection, systemic administration allows for more homogeneous microdistribution. Moreover, systemic administration allows for sufficient washout time to elapse, to allow for the elimination of non-specific fluorescence from the blood and the urinary tract (22). In contrast to intra-tumoral injection, systemic administration also allows the detection of previously unrecognized tumor foci or metastases.

Few of these mAb-based fluorescent probes have progressed into clinical testing. One that did, a first-in-human clinical trial of fluorescence-guided navigation to aid surgery in head and neck cancers is currently underway. This trial utilizes the anti-EGFR antibody conjugate, cetuximab-IRDye800CW for use in head and neck cancers (94, 95). In this trial, Rosenthal et al. demonstrated

that the EGFR mAb-fluorophore conjugate was both safe and effective. The target-to-background ratio (TBR) achieved in this study (mean TBR of 5.2 in the highest dose range) improved the accuracy of surgical decision-making (95). Recently, cetuximab-IRDye800CW or bevacizumab-IRDye800CW (targeting vascular endothelial growth factor)-have also been in clinical trials targeting pancreatic adenocarcinoma, colon cancer, and breast cancer (102, 126). It was noted that the conjugation of the IRDye800CW significantly shortened the circulating half-life of cetuximab despite a low antibody-to-dye conjugation ratio (approximately 1) (95). Rapid clearance of mAb–dye conjugates can help lower the background signal; however, it can simultaneously compromise tumor accumulation. Taken together, these alterations could lower the overall performance of the agent.

Another exciting advancement with potential implications for FGS is a technique called "near infrared photoimmunotherapy" (NIR-PIT) (96). NIR-PIT is based on an antibody that targets a cell-surface antigen but is conjugated to a photoabsorbing dye (IRDye700DX) that has both fluorescent characteristics and the ability to damage cells to which it has conjugated. Thus, NIR-PIT has the dual ability to localize tumors and as well as selectively eliminate cancer cells. The cytotoxic effects of NIR-PIT are observed only when the mAb-IR700 conjugate is bound to receptors on the cell membrane; no phototoxicity is observed when the conjugate is present but not yet bound (96). Therefore, NIR-PIT achieves highly selected targeted cancer cell killing. NIR-PIT has been shown to be effective in a variety of different cancer cell types exhibiting a range of surface antigens such as EGFR, CD20, mesothelin, and PSMA (198–202). Furthermore, a first-in-human phase 2 trial of NIR-PIT in patients with inoperable head and neck cancer was recently completed and the agent is being commercialized. NIR-PIT has great potential as a new cancer treatment for many tumor types when combined with FGS.

These fluorescence imaging probes, including IRDye700DX and IRDye800CW, typically result in an "always-on" type of fluorescence signal. Therefore, fluorescence in the cancer tissues is roughly related to the amount of conjugated mAb bound to the tumor. By showing sufficient expression of target molecules, activatable fluorescent probes would be useful for selecting eligible patients who could be efficiently treated with FGS.

Activatable Fluorescent Probes

Based on pharmacokinetics, the "perfect" *in vivo* targeting agent has not yet been developed. The fundamental disadvantage of "always-on" probes is that they emit signal regardless of their proximity or interaction with the target tissues. As a result, there is considerable background signal to contend with. In order to design superior molecular imaging probes, one seeks to either (1) maximize signal from the target, (2) minimize signal from the background, or (3) do both. All lead to improved TBR, which, in turn, improves the sensitivity and specificity for detecting tumors with imaging (203).

Activatable fluorescent probes ("smart probes") target tumor cells by taking advantage of the physiologic differences between cancerous and normal cells, thus enhancing tumor margin detection (204). Because activatable probes do not emit signals before engaging the target, unbound probes do not yield a signal. Therefore, there is less background signal to compromise the sensitivity and specificity, yielding an absolute increase in TBR (205). Consequently, compared with "always-on" fluorescent probes, activatable fluorescent probes have a higher TBR (203). Preclinical studies have shown the merits of this approach (206–208). For example, when employing the antibody as a platform for activatable imaging probes, IgG-based activatable probes typically yield both the highest signal (due to high binding) as well as highest TBR (due to absent background signal) compared with "always-on" probes (203, 209, 210) (**Figure 1**).

There are two basic types of activatable fluorescent probes (**Figure 2**) (203, 207, 211). One type is enzyme reactive activatable fluorescent probe, which exist in the quenched state until they are activated by enzymatic cleavage mostly outside of the cells (212, 213) (**Figure 2**). Well known targeted enzymes are cathepsin, matrix metalloproteinases (MMP), γ-glutamyltransferase (GGT), and beta-galactosidases. Some of enzyme reactive activatable fluorescent probes can be topically or locally applied.

Another type of activatable fluorescent probe is molecular-binding activatable fluorescent probes, which are quenched until activated in targeted cells by endolysosomal processing (**Figure 2**). Within the lysosome, catabolism can occur under conditions such as low pH, protease activity, or oxidation, which

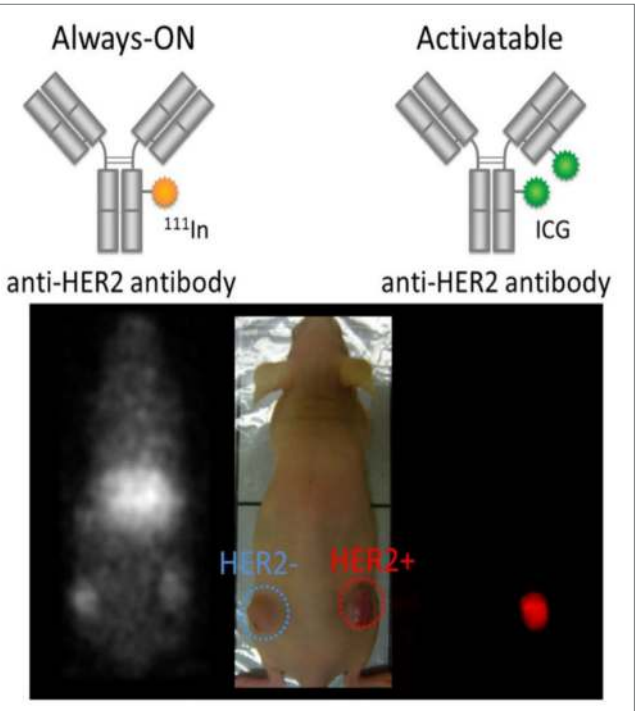

FIGURE 1 | Comparison of molecularly targeted fluorescent probes using always-on and activatable fluorescence strategies. Radiolabeled trastuzumab targeting HER2 with always-on fluorophores depicts both bound and unbound agents (left and right tumors) resulting in poor target-to-background ratio (TBR). In contrast, the activatable fluorescent probe, indocyanine green (ICG)-labeled trastuzumab, depicts only HER2-expressing tumors (right tumor) without incurring background signal resulting in superior TBR. Reprinted from publication (210) with permission from Elsevier.

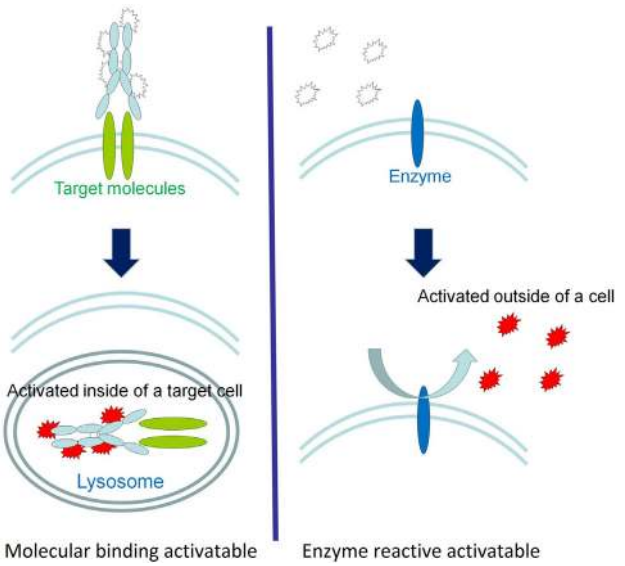

FIGURE 2 | A schematic explanation of the two types of activatable fluorescence probes. The fluorescence activation of molecularly targeted activatable probes occurs intracellularly (left), whereas enzyme reactive activation typically occurs in the extracellular environment (right). Reprinted with permission from Ref. (203). Copyright 2011 American Chemical Society.

can release the fluorophore from its quenched state. For example, a pH-activatable fluorescent probe produces light only in tumors due to their acidic microenvironment, resulting in high TBR whereas control "always-on" probes produce lower TBR due to higher background signal (**Figure 3**) (155, 214). This type of activatable fluorescent probe is administered systematically *via* intravenous injection.

There are advantages and disadvantages to both methods. In enzymatic activation, a single target enzyme can activate many different fluorescent molecules, thus amplifying the signal from the target tissue. However, a disadvantage of enzymatic activation is that the activation occurs in the extracellular space and the enzyme may diffuse away from the target contributing to background signal. Furthermore, this type of probe lacks specificity because none of the currently utilized enzymes for fluorescence activation are specific for carcinogenesis. In contrast, probes that are activated by endolysosomal processing, are highly specific for cancer and generally remain localized to the target as activation relies upon the probe binding specific cell-surface receptors and being internalized. However, molecular-binding of specific activatable fluorescent probes requires a biological and catabolic process to gain sufficient TBR. Targeted activatable fluorescent probes need to first leak from the vasculature, bind target cells, and then internalize within the target cell to activate the probe. The activation process often requires days, which decreases their practicality for routine clinical use (214). Novel activatable fluorescent probes targeting additional physiologic characteristics of cancer cells, such as degradation of the micelle, thiol concentration, surface lectins, and antibody binding, are also currently in development (159, 207, 211, 215–218). Translating these activatable fluorescent probes into clinical studies could significantly increase the number and quality of intraoperative imaging tools available during cancer excision.

Activatable fluorescent probes vary greatly by the mechanism by which fluorescence is quenched. The best known quenching mechanism is Föster (fluorescence) resonance energy transfer (FRET), wherein energy from one fluorophore is transferred to another molecule when the two molecules are in close (<10 nm) proximity. The FRET pair can consist of two fluorophores (self-quenching) or a fluorophore and a quencher molecule (203, 219). Homo-dimer (H or J-dimer) formation is other method of quenching. For instance, xanthene derivatives are known to form H-dimers at higher concentrations (~mM) which induces shifts of absorbance spectra, completely quenching fluorescence (195, 203). Fundamental to both FRET and H-dimer formation is the inter-fluorophore processing that occurs when the two molecules are in proximity to each other.

Another quenching mechanism, photon induced electron transfer (PeT) occurs when an electron is transfered from the PeT donor to the excited fluorophore diminishing the fluorescence signal. When the PeT donor is cleaved from the fluorophore or inactivated, activation occurs. Unlike FRET and H-dimer formation, PeT occurs within a single fluorophore molecule and does not require the presence of a second fluorophore (203, 220). The PeT mechanism has a particularly high dequench:quench light ratio.

Yet another mechanism of dequenching is to hold two fluorophores in close proximity to each other using a peptide backbone. In the presence of an enzyme the peptide backbone is cleaved releasing and activating the fluorophores.

The first activatable fluorescent probe to be tested in clinical trials was LUM015. The activation of LUM015 relied on cleavage by a cathepsin protease, an enzyme commonly overexpressed by tumors (221). LUM015 is optically inactive under normal conditions, but upon proteolytic cleavage, a covalently attached quencher molecule is released and fluorescence signal greatly intensifies (103). It was first evaluated by Whitley et al. in a cohort of 15 patients with breast cancer or soft-tissue sarcoma (103). Intravenous injection of this protease-activated fluorescent imaging probe before surgery was well tolerated, and imaging of resected human tissues showed that fluorescence from the tumor was significantly higher than fluorescence from normal tissues (103).

Recently, several other mechanisms have been tested. A quenched activatable cell-penetrating peptide, AVB-620 was tested in a first-in-human clinical trial in which 27 breast cancer patients received the infusion followed by surgical excision. Infusion of AVB-620 was safe and improved intraoperative cancer detection (104). Another new approach is to use peptide conjugated to ICG. In this case the agent, BLZ-100, uses chlorotoxin (36-amino acid peptide) as the targeting moiety and conjugates it to ICG. This agent has been used for glioma imaging (90).

Sprayable Activatable Fluorescent Probes

In many cases, the dequenching process takes hours to days making it problematic for integration into surgical workflows.

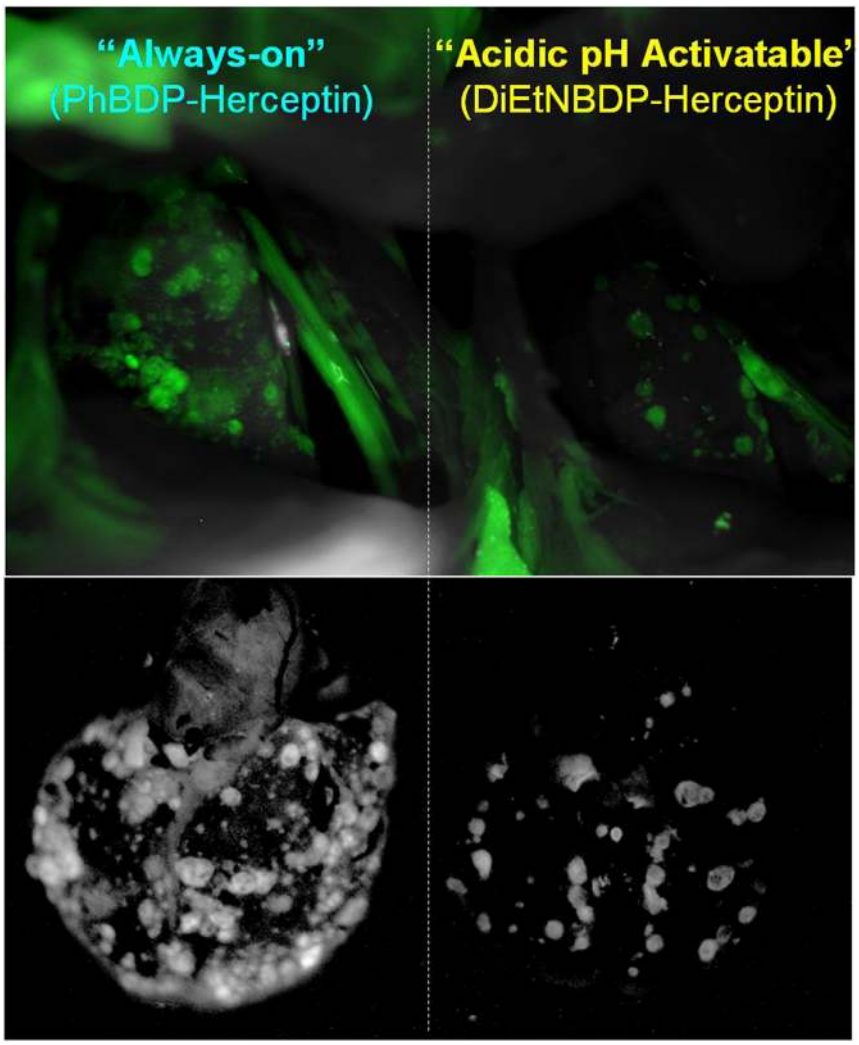

FIGURE 3 | *In vivo* tumor detection with targeted activatable fluorescent probes in a HER2-positive lung metastasis model mice. The pH-activatable fluorescent probe produces light only in tumors in the lung. However, the control "always-on" probe produces fluorescent signal from both tumors and normal lung and heart reducing the tumor to background ratio. Reprinted with permission from Ref. (155). Copyright 2010 American Chemical Society.

For instance, activatable probes using cathepsin D and MMP2/9 (222, 223), should be systemically injected at least a day before the surgery to be delivered to cancer and fully activated because of multiple cleavage sites. However, the kinetics of some other enzyme reactive probes is much faster especially when activated by a single cleavage. Therefore, such enzymatically activatable fluorescent probes can be so fast as to be used as needed during a surgical procedure. For instance, Urano et al. developed the activatable fluorescent probe, γ-glutamyl hydroxymethyl rhodamine green (gGlu-HMRG). The gGlu-HMRG is completely quenched by spirocyclic caging, but is activated rapidly with a one-step enzymatic reaction in the presence of GGT which is often present on cell membranes of cervical and ovarian cancer cells. As a result, this probe activates within 10 min of it being sprayed on. In a mouse model of human ovarian cancer, Urano et al. sprayed the abdominal cavity with the gGlu-HMRG probe and demonstrated that small tumor nodules could be visualized within 10 min after administration and remained labeled for at least 1 h (**Figure 4**) (112). Mitsunaga et al. used gGlu-HMRG during colonoscopy to differentiate long-term colitis from early colitis-associated cancer in a mouse colon cancer mouse model. They were able to visualize cancers and dysplasia 5–30 min after spraying gGlu-HMRG on the colon surface. Moreover, signal from cancer/dysplasia was 10 times higher than background fluorescence despite the presence of colitis (127). gGlu-HMRG probe has recently been tested in fresh human surgical specimens of colorectal tumor (224) and breast cancer (225) for detecting tumor borders and metastatic lymph nodes as a precursor to it being introduced in clinical trials. Similarly, these probes revealed that topical administration of the agent on aspirated specimens from patients with pancreatic tumors resulted in tumor-specific enhancement (226).

Other sprayable activatable probes are in development. These are activated by enzymes by a single cleavage such as cathepsin

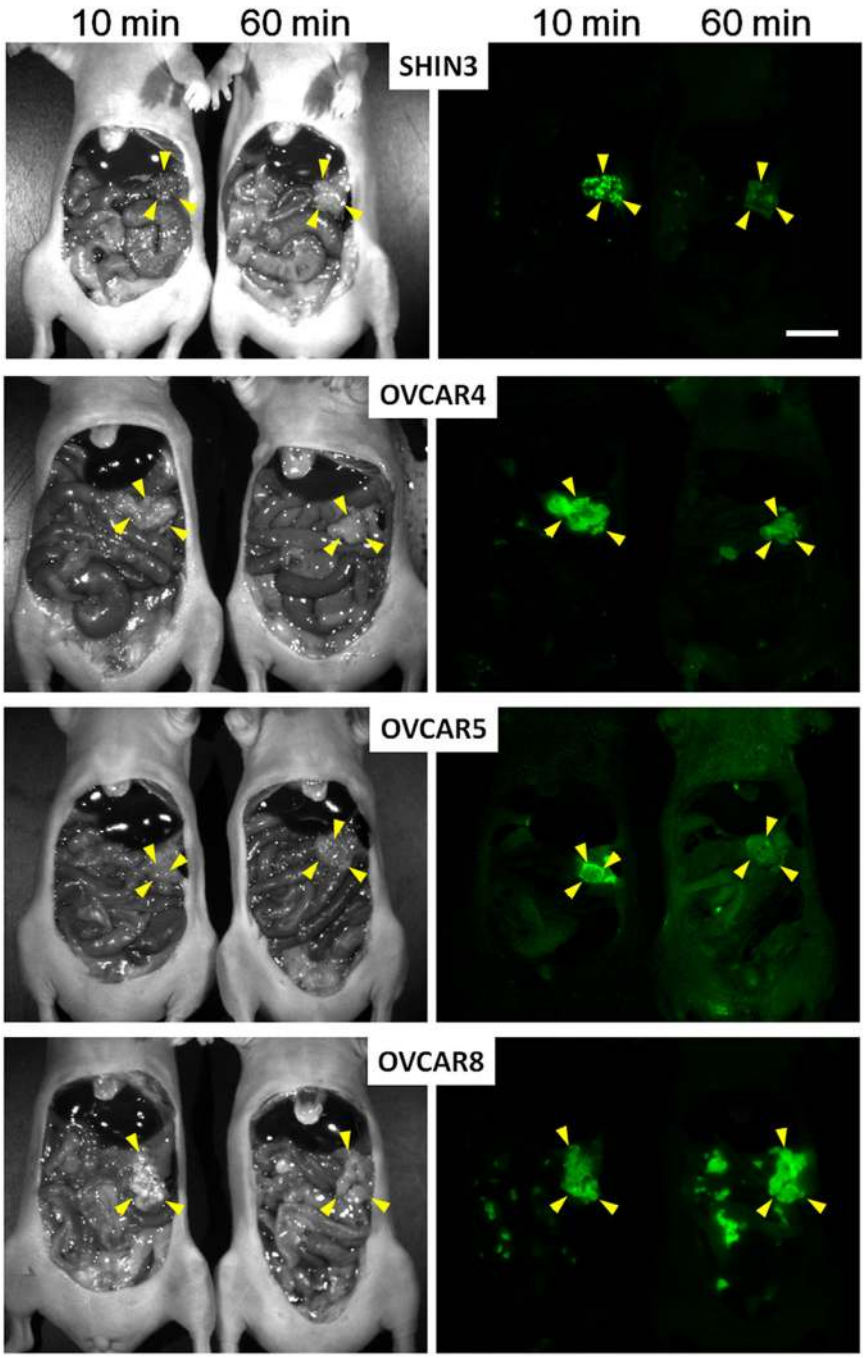

FIGURE 4 | Spectral fluorescence images of four peritoneal ovarian cancers using gGlu-HMRG. *In vivo* fluorescence intensity of a sprayable probe. By 10 and 60 min after intraperitoneal gGlu-HMRG administration each of four peritoneal ovarian tumor models: SHIN3, OVCAR4, OVCAR5, and OVCAR8 were evaluated. Yellow arrowheads indicate tumor location. Scale bar, 1 cm. Reprinted from publication (112) with permission from AAAS.

(91, 129), beta-galactosidase (227), endo-aminopeptidases (228), and NADPH (229).

The various types of recently developed activatable fluorescent probes tend to be superior to always-on probes; however, their safety in patients is yet to be determined. Given the relatively small market, bringing such agents thru the approval process to a New Drug Application will be challenging.

SUMMARY

The limits of white light imaging during surgical and endoscopic procedures are well known. It is acknowledged that current optical methods tend to have insufficient sensitivity for small tumors and do poorly at determining tumor margins. Targeted fluorescence imaging can provide additional information that

augments the ability of the operator to see and treat pathology, thus lowering the rate of persistent or recurrent disease. FGS, because of its high sensitivity, low cost, portability and real-time capabilities, has great potential to improve surgical outcomes. Not only can this approach direct intraoperative image guidance for surgical margin assessments but can also help surgeons detect microscopic tumors or residual lesions that may have otherwise been missed. In addition, anatomical fluorescence imaging techniques can aid in avoiding complications in various surgical situations. Despite the availability of these technologies, most surgeons still rely largely on visual and tactile cues combined with presurgical radiologic imaging to guide tissue resection.

As techniques continue to improve, FGS will move toward the concept of "precision surgical therapy." It is possible that FGS will be personally designed for each patient's specific disease process. Although much more work is necessary to reach this goal, in the meantime there is a rapidly expanding number of targeted fluorescence imaging probes that offer great potential for the future. Hopefully, these advances will enable FGS to become more widely available for a broad range of cancer types.

AUTHOR CONTRIBUTIONS

All authors listed have made a substantial, direct, and intellectual contribution to the work and approved it for publication.

ACKNOWLEDGMENTS

This review was supported by the Intramural Research Program of the NIH, National Cancer Institute, Center for Cancer Research (ZIA BC 011512).

REFERENCES

1. DeSantis CE, Lin CC, Mariotto AB, Siegel RL, Stein KD, Kramer JL, et al. Cancer treatment and survivorship statistics, 2014. *CA Cancer J Clin* (2014) 64(4):252–71. doi:10.3322/caac.21235
2. Haque R, Contreras R, McNicoll MP, Eckberg EC, Petitti DB. Surgical margins and survival after head and neck cancer surgery. *BMC Ear Nose Throat Disord* (2006) 6:2. doi:10.1186/1472-6815-6-2
3. Singletary SE. Surgical margins in patients with early-stage breast cancer treated with breast conservation therapy. *Am J Surg* (2002) 184(5):383–93. doi:10.1016/S0002-9610(02)01012-7
4. Meric F, Mirza NQ, Vlastos G, Buchholz TA, Kuerer HM, Babiera GV, et al. Positive surgical margins and ipsilateral breast tumor recurrence predict disease-specific survival after breast-conserving therapy. *Cancer* (2003) 97(4):926–33. doi:10.1002/cncr.11222
5. Snijder RJ, Brutel de la Riviere A, Elbers HJ, van den Bosch JM. Survival in resected stage I lung cancer with residual tumor at the bronchial resection margin. *Ann Thorac Surg* (1998) 65(1):212–6. doi:10.1016/S0003-4975(97)01114-4
6. Nagtegaal ID, Quirke P. What is the role for the circumferential margin in the modern treatment of rectal cancer? *J Clin Oncol* (2008) 26(2):303–12. doi:10.1200/jco.2007.12.7027
7. Dotan ZA, Kavanagh K, Yossepowitch O, Kaag M, Olgac S, Donat M, et al. Positive surgical margins in soft tissue following radical cystectomy for bladder cancer and cancer specific survival. *J Urol* (2007) 178(6):2308–12; discussion 2313. doi:10.1016/j.juro.2007.08.023
8. Wieder JA, Soloway MS. Incidence, etiology, location, prevention and treatment of positive surgical margins after radical prostatectomy for prostate cancer. *J Urol* (1998) 160(2):299–315. doi:10.1097/00005392-199808000-00003
9. Rosenthal EL, Warram JM, Bland KI, Zinn KR. The status of contemporary image-guided modalities in oncologic surgery. *Ann Surg* (2015) 261(1):46–55. doi:10.1097/sla.0000000000000622
10. Ravasz LA, Slootweg PJ, Hordijk GJ, Smit F, van der Tweel I. The status of the resection margin as a prognostic factor in the treatment of head and neck carcinoma. *J Craniomaxillofac Surg* (1991) 19(7):314–8. doi:10.1016/S1010-5182(05)80339-7
11. Choti MA, Sitzmann JV, Tiburi MF, Sumetchotimetha W, Rangsin R, Schulick RD, et al. Trends in long-term survival following liver resection for hepatic colorectal metastases. *Ann Surg* (2002) 235(6):759–66. doi:10.1097/00000658-200206000-00002
12. McMahon J, O'Brien CJ, Pathak I, Hamill R, McNeil E, Hammersley N, et al. Influence of condition of surgical margins on local recurrence and disease-specific survival in oral and oropharyngeal cancer. *Br J Oral Maxillofac Surg* (2003) 41(4):224–31. doi:10.1016/S0266-4356(03)00119-0
13. Woolgar JA, Triantafyllou A. A histopathological appraisal of surgical margins in oral and oropharyngeal cancer resection specimens. *Oral Oncol* (2005) 41(10):1034–43. doi:10.1016/j.oraloncology.2005.06.008
14. Iczkowski KA, Lucia MS. Frequency of positive surgical margin at prostatectomy and its effect on patient outcome. *Prostate Cancer* (2011) 2011:673021. doi:10.1155/2011/673021
15. Atkins J, Al Mushawah F, Appleton CM, Cyr AE, Gillanders WE, Aft RL, et al. Positive margin rates following breast-conserving surgery for stage I-III breast cancer: palpable versus nonpalpable tumors. *J Surg Res* (2012) 177(1):109–15. doi:10.1016/j.jss.2012.03.045
16. Chagpar AB. Cavity shave margins in breast cancer. *N Engl J Med* (2015) 373(22):2187–8. doi:10.1056/NEJMc1511344
17. Rosenthal EL, Warram JM, de Boer E, Basilion JP, Biel MA, Bogyo M, et al. Successful translation of fluorescence navigation during oncologic surgery: a consensus report. *J Nucl Med* (2016) 57(1):144–50. doi:10.2967/jnumed.115.158915
18. Kubben PL, ter Meulen KJ, Schijns OE, ter Laak-Poort MP, van Overbeeke JJ, van Santbrink H. Intraoperative MRI-guided resection of glioblastoma multiforme: a systematic review. *Lancet Oncol* (2011) 12(11):1062–70. doi:10.1016/s1470-2045(11)70130-9
19. Li L, Wang P, Chen L, Ma X, Bu B, Yu X. Individualized treatment of craniovertebral junction malformation guided by intraoperative computed tomography. *J Spinal Disord Tech* (2012) 25(2):77–84. doi:10.1097/BSD.0b013e31820f8afb
20. Singh H, Rote S, Jada A, Bander ED, Almodovar-Mercado GJ, Essayed WI, et al. Endoscopic endonasal odontoid resection with real-time intraoperative image-guided computed tomography: report of 4 cases. *J Neurosurg* (2017):1–6. doi:10.3171/2017.1.jns162601
21. Moore GE, Peyton WT. The clinical use of fluorescein in neurosurgery; the localization of brain tumors. *J Neurosurg* (1948) 5(4):392–8. doi:10.3171/jns.1948.5.4.0392
22. Nguyen QT, Tsien RY. Fluorescence-guided surgery with live molecular navigation – a new cutting edge. *Nat Rev Cancer* (2013) 13(9):653–62. doi:10.1038/nrc3566
23. Vahrmeijer AL, Hutteman M, van der Vorst JR, van de Velde CJ, Frangioni JV. Image-guided cancer surgery using near-infrared fluorescence. *Nat Rev Clin Oncol* (2013) 10(9):507–18. doi:10.1038/nrclinonc.2013.123
24. DeLong JC, Hoffman RM, Bouvet M. Current status and future perspectives of fluorescence-guided surgery for cancer. *Expert Rev Anticancer Ther* (2016) 16(1):71–81. doi:10.1586/14737140.2016.1121109
25. Alander JT, Kaartinen I, Laakso A, Patila T, Spillmann T, Tuchin VV, et al. A review of indocyanine green fluorescent imaging in surgery. *Int J Biomed Imaging* (2012) 2012:940585. doi:10.1155/2012/940585
26. Xi L, Jiang H. Image-guided surgery using multimodality strategy and molecular probes. *Wiley Interdiscip Rev Nanomed Nanobiotechnol* (2016) 8(1):46–60. doi:10.1002/wnan.1352
27. AV DS, Lin H, Henderson ER, Samkoe KS, Pogue BW. Review of fluorescence guided surgery systems: identification of key performance capabilities beyond indocyanine green imaging. *J Biomed Opt* (2016) 21(8):80901. doi:10.1117/1.jbo.21.8.080901

28. van Dam GM, Themelis G, Crane LM, Harlaar NJ, Pleijhuis RG, Kelder W, et al. Intraoperative tumor-specific fluorescence imaging in ovarian cancer by folate receptor-alpha targeting: first in-human results. *Nat Med* (2011) 17(10):1315–9. doi:10.1038/nm.2472
29. Aldave G, Tejada S, Pay E, Marigil M, Bejarano B, Idoate MA, et al. Prognostic value of residual fluorescent tissue in glioblastoma patients after gross total resection in 5-aminolevulinic acid-guided surgery. *Neurosurgery* (2013) 72(6):915–20; discussion 920–1. doi:10.1227/NEU.0b013e31828c3974
30. Hussain T, Nguyen QT. Molecular imaging for cancer diagnosis and surgery. *Adv Drug Deliv Rev* (2014) 66:90–100. doi:10.1016/j.addr.2013.09.007
31. de Boer E, Harlaar NJ, Taruttis A, Nagengast WB, Rosenthal EL, Ntziachristos V, et al. Optical innovations in surgery. *Br J Surg* (2015) 102(2):e56–72. doi:10.1002/bjs.9713
32. Lee BT, Hutteman M, Gioux S, Stockdale A, Lin SJ, Ngo LH, et al. The FLARE intraoperative near-infrared fluorescence imaging system: a first-in-human clinical trial in perforator flap breast reconstruction. *Plast Reconstr Surg* (2010) 126(5):1472–81. doi:10.1097/PRS.0b013e3181f059c7
33. Hill TK, Mohs AM. Image-guided tumor surgery: will there be a role for fluorescent nanoparticles? *Wiley Interdiscip Rev Nanomed Nanobiotechnol* (2016) 8(4):498–511. doi:10.1002/wnan.1381
34. Motomura K, Inaji H, Komoike Y, Kasugai T, Noguchi S, Koyama H. Sentinel node biopsy guided by indocyanine green dye in breast cancer patients. *Jpn J Clin Oncol* (1999) 29(12):604–7. doi:10.1093/jjco/29.12.604
35. Kitai T, Inomoto T, Miwa M, Shikayama T. Fluorescence navigation with indocyanine green for detecting sentinel lymph nodes in breast cancer. *Breast Cancer* (2005) 12(3):211–5. doi:10.2325/jbcs.12.211
36. Tagaya N, Yamazaki R, Nakagawa A, Abe A, Hamada K, Kubota K, et al. Intraoperative identification of sentinel lymph nodes by near-infrared fluorescence imaging in patients with breast cancer. *Am J Surg* (2008) 195(6):850–3. doi:10.1016/j.amjsurg.2007.02.032
37. Murawa D, Hirche C, Dresel S, Hunerbein M. Sentinel lymph node biopsy in breast cancer guided by indocyanine green fluorescence. *Br J Surg* (2009) 96(11):1289–94. doi:10.1002/bjs.6721
38. Zakaria S, Hoskin TL, Degnim AC. Safety and technical success of methylene blue dye for lymphatic mapping in breast cancer. *Am J Surg* (2008) 196(2):228–33. doi:10.1016/j.amjsurg.2007.08.060
39. Peek MC, Charalampoudis P, Anninga B, Baker R, Douek M. Blue dye for identification of sentinel nodes in breast cancer and malignant melanoma: a systematic review and meta-analysis. *Future Oncol* (2017) 13(5):455–67. doi:10.2217/fon-2016-0255
40. Fujiwara M, Mizukami T, Suzuki A, Fukamizu H. Sentinel lymph node detection in skin cancer patients using real-time fluorescence navigation with indocyanine green: preliminary experience. *J Plast Reconstr Aesthet Surg* (2009) 62(10):e373–8. doi:10.1016/j.bjps.2007.12.074
41. Tanaka R, Nakashima K, Fujimoto W. Sentinel lymph node detection in skin cancer using fluorescence navigation with indocyanine green. *J Dermatol* (2009) 36(8):468–70. doi:10.1111/j.1346-8138.2009.00679.x
42. Bredell MG. Sentinel lymph node mapping by indocyanin green fluorescence imaging in oropharyngeal cancer – preliminary experience. *Head Neck Oncol* (2010) 2:31. doi:10.1186/1758-3284-2-31
43. Yamashita S, Tokuishi K, Anami K, Miyawaki M, Moroga T, Kamei M, et al. Video-assisted thoracoscopic indocyanine green fluorescence imaging system shows sentinel lymph nodes in non-small-cell lung cancer. *J Thorac Cardiovasc Surg* (2011) 141(1):141–4. doi:10.1016/j.jtcvs.2010.01.028
44. Yuasa Y, Seike J, Yoshida T, Takechi H, Yamai H, Yamamoto Y, et al. Sentinel lymph node biopsy using intraoperative indocyanine green fluorescence imaging navigated with preoperative CT lymphography for superficial esophageal cancer. *Ann Surg Oncol* (2012) 19(2):486–93. doi:10.1245/s10434-011-1922-x
45. Kubota K, Yoshida M, Kuroda J, Okada A, Ohta K, Kitajima M. Application of the HyperEye Medical System for esophageal cancer surgery: a preliminary report. *Surg Today* (2013) 43(2):215–20. doi:10.1007/s00595-012-0251-4
46. Nimura H, Narimiya N, Mitsumori N, Yamazaki Y, Yanaga K, Urashima M. Infrared ray electronic endoscopy combined with indocyanine green injection for detection of sentinel nodes of patients with gastric cancer. *Br J Surg* (2004) 91(5):575–9. doi:10.1002/bjs.4470
47. Kusano M, Tajima Y, Yamazaki K, Kato M, Watanabe M, Miwa M. Sentinel node mapping guided by indocyanine green fluorescence imaging: a new method for sentinel node navigation surgery in gastrointestinal cancer. *Dig Surg* (2008) 25(2):103–8. doi:10.1159/000121905
48. Noura S, Ohue M, Seki Y, Tanaka K, Motoori M, Kishi K, et al. Feasibility of a lateral region sentinel node biopsy of lower rectal cancer guided by indocyanine green using a near-infrared camera system. *Ann Surg Oncol* (2010) 17(1):144–51. doi:10.1245/s10434-009-0711-2
49. Hirche C, Dresel S, Krempien R, Hunerbein M. Sentinel node biopsy by indocyanine green retention fluorescence detection for inguinal lymph node staging of anal cancer: preliminary experience. *Ann Surg Oncol* (2010) 17(9):2357–62. doi:10.1245/s10434-010-1010-7
50. Jeschke S, Lusuardi L, Myatt A, Hruby S, Pirich C, Janetschek G. Visualisation of the lymph node pathway in real time by laparoscopic radioisotope- and fluorescence-guided sentinel lymph node dissection in prostate cancer staging. *Urology* (2012) 80(5):1080–6. doi:10.1016/j.urology.2012.05.050
51. Polom W, Markuszewski M, Rho YS, Matuszewski M. Usage of invisible near infrared light (NIR) fluorescence with indocyanine green (ICG) and methylene blue (MB) in urological oncology. Part 1. *Cent European J Urol* (2014) 67(2):142–8. doi:10.5173/ceju.2014.02.art5
52. Polom W, Markuszewski M, Rho YS, Matuszewski M. Use of invisible near infrared light fluorescence with indocyanine green and methylene blue in urology. Part 2. *Cent European J Urol* (2014) 67(3):310–3. doi:10.5173/ceju.2014.03.art19
53. Ogata F, Narushima M, Mihara M, Azuma R, Morimoto Y, Koshima I. Intraoperative lymphography using indocyanine green dye for near-infrared fluorescence labeling in lymphedema. *Ann Plast Surg* (2007) 59(2):180–4. doi:10.1097/01.sap.0000253341.70866.54
54. Unno N, Inuzuka K, Suzuki M, Yamamoto N, Sagara D, Nishiyama M, et al. Preliminary experience with a novel fluorescence lymphography using indocyanine green in patients with secondary lymphedema. *J Vasc Surg* (2007) 45(5):1016–21. doi:10.1016/j.jvs.2007.01.023
55. Chang DW, Suami H, Skoracki R. A prospective analysis of 100 consecutive lymphovenous bypass cases for treatment of extremity lymphedema. *Plast Reconstr Surg* (2013) 132(5):1305–14. doi:10.1097/PRS.0b013e3182a4d626
56. Kuroda K, Kinouchi H, Kanemaru K, Nishiyama Y, Ogiwara M, Yoshioka H, et al. Intra-arterial injection fluorescein videoangiography in aneurysm surgery. *Neurosurgery* (2013) 72(2 Suppl Operative):ons141–50; discussion ons150. doi:10.1227/NEU.0b013e3182752f32
57. Ichikawa T, Suzuki K, Watanabe Y. Intra-arterial fluorescence angiography with injection of fluorescein sodium from the superficial temporal artery during aneurysm surgery: technical notes. *Neurol Med Chir (Tokyo)* (2014) 54(6):490–6. doi:10.2176/nmc.tn.2013-0232
58. Ichikawa T, Suzuki K, Watanabe Y, Sato T, Sakuma J, Saito K. Development of and clinical experience with a simple device for performing intraoperative fluorescein fluorescence cerebral angiography: technical notes. *Neurol Med Chir (Tokyo)* (2016) 56(3):141–9. doi:10.2176/nmc.tn.2015-0188
59. Yamamoto M, Sasaguri S, Sato T. Assessing intraoperative blood flow in cardiovascular surgery. *Surg Today* (2011) 41(11):1467–74. doi:10.1007/s00595-010-4553-0
60. Yamamoto M, Orihashi K, Nishimori H, Handa T, Kondo N, Fukutomi T, et al. Efficacy of intraoperative HyperEye Medical System angiography for coronary artery bypass grafting. *Surg Today* (2015) 45(8):966–72. doi:10.1007/s00595-014-1015-0
61. Yamamoto M, Orihashi K, Nishimori H, Wariishi S, Fukutomi T, Kondo N, et al. Indocyanine green angiography for intra-operative assessment in vascular surgery. *Eur J Vasc Endovasc Surg* (2012) 43(4):426–32. doi:10.1016/j.ejvs.2011.12.030
62. Jafari MD, Lee KH, Halabi WJ, Mills SD, Carmichael JC, Stamos MJ, et al. The use of indocyanine green fluorescence to assess anastomotic perfusion during robotic assisted laparoscopic rectal surgery. *Surg Endosc* (2013) 27(8):3003–8. doi:10.1007/s00464-013-2832-8
63. Pacheco PE, Hill SM, Henriques SM, Paulsen JK, Anderson RC. The novel use of intraoperative laser-induced fluorescence of indocyanine green tissue angiography for evaluation of the gastric conduit in esophageal reconstructive surgery. *Am J Surg* (2013) 205(3):349–52; discussion 352–3. doi:10.1016/j.amjsurg.2012.11.005
64. Yamaguchi S, De Lorenzi F, Petit JY, Rietjens M, Garusi C, Giraldo A, et al. The "perfusion map" of the unipedicled TRAM flap to reduce postoperative

partial necrosis. *Ann Plast Surg* (2004) 53(3):205–9. doi:10.1097/01.sap.0000116284.51679.ea
65. Giunta RE, Holzbach T, Taskov C, Holm PS, Brill T, Busch R, et al. Prediction of flap necrosis with laser induced indocyanine green fluorescence in a rat model. *Br J Plast Surg* (2005) 58(5):695–701. doi:10.1016/j.bjps.2005.02.018
66. Holm C, Mayr M, Hofter E, Raab N, Ninkovic M. Interindividual variability of the SIEA angiosome: effects on operative strategies in breast reconstruction. *Plast Reconstr Surg* (2008) 122(6):1612–20. doi:10.1097/PRS.0b013e31818a9a3f
67. Lamby P, Prantl L, Gais S, Walter M, Bachthaler M, Nerlich M, et al. Evaluation of the vascular integrity of free flaps based on microcirculation imaging techniques. *Clin Hemorheol Microcirc* (2008) 39(1–4):253–63. doi:10.3233/CH-2008-1094
68. Newman MI, Samson MC. The application of laser-assisted indocyanine green fluorescent dye angiography in microsurgical breast reconstruction. *J Reconstr Microsurg* (2009) 25(1):21–6. doi:10.1055/s-0028-1090617
69. Pestana IA, Coan B, Erdmann D, Marcus J, Levin LS, Zenn MR. Early experience with fluorescent angiography in free-tissue transfer reconstruction. *Plast Reconstr Surg* (2009) 123(4):1239–44. doi:10.1097/PRS.0b013e31819e67c1
70. Komorowska-Timek E, Gurtner GC. Intraoperative perfusion mapping with laser-assisted indocyanine green imaging can predict and prevent complications in immediate breast reconstruction. *Plast Reconstr Surg* (2010) 125(4):1065–73. doi:10.1097/PRS.0b013e3181d17f80
71. Ishizawa T, Bandai Y, Ijichi M, Kaneko J, Hasegawa K, Kokudo N. Fluorescent cholangiography illuminating the biliary tree during laparoscopic cholecystectomy. *Br J Surg* (2010) 97(9):1369–77. doi:10.1002/bjs.7125
72. Boni L, David G, Mangano A, Dionigi G, Rausei S, Spampatti S, et al. Clinical applications of indocyanine green (ICG) enhanced fluorescence in laparoscopic surgery. *Surg Endosc* (2015) 29(7):2046–55. doi:10.1007/s00464-014-3895-x
73. Winer JH, Choi HS, Gibbs-Strauss SL, Ashitate Y, Colson YL, Frangioni JV. Intraoperative localization of insulinoma and normal pancreas using invisible near-infrared fluorescent light. *Ann Surg Oncol* (2010) 17(4):1094–100. doi:10.1245/s10434-009-0868-8
74. Wada H, Hyun H, Vargas C, Gravier J, Park G, Gioux S, et al. Pancreas-targeted NIR fluorophores for dual-channel image-guided abdominal surgery. *Theranostics* (2015) 5(1):1–11. doi:10.7150/thno.10259
75. Verbeek FP, van der Vorst JR, Schaafsma BE, Swijnenburg RJ, Gaarenstroom KN, Elzevier HW, et al. Intraoperative near infrared fluorescence guided identification of the ureters using low dose methylene blue: a first in human experience. *J Urol* (2013) 190(2):574–9. doi:10.1016/j.juro.2013.02.3187
76. Whitney MA, Crisp JL, Nguyen LT, Friedman B, Gross LA, Steinbach P, et al. Fluorescent peptides highlight peripheral nerves during surgery in mice. *Nat Biotechnol* (2011) 29(4):352–6. doi:10.1038/nbt.1764
77. Wu AP, Whitney MA, Crisp JL, Friedman B, Tsien RY, Nguyen QT. Improved facial nerve identification with novel fluorescently labeled probe. *Laryngoscope* (2011) 121(4):805–10. doi:10.1002/lary.21411
78. Hyun H, Park MH, Owens EA, Wada H, Henary M, Handgraaf HJ. Structure-inherent targeting of near-infrared fluorophores for parathyroid and thyroid gland imaging. *Nat Med* (2015) 21(2):192–7. doi:10.1038/nm.3728
79. Owens EA, Hyun H, Tawney JG, Choi HS, Henary M. Correlating molecular character of NIR imaging agents with tissue-specific uptake. *J Med Chem* (2015) 58(10):4348–56. doi:10.1021/acs.jmedchem.5b00475
80. Ashitate Y, Levitz A, Park MH, Hyun H, Venugopal V, Park G, et al. Endocrine-specific NIR fluorophores for adrenal gland targeting. *Chem Commun (Camb)* (2016) 52(67):10305–8. doi:10.1039/c6cc03845j
81. Owens EA, Hyun H, Dost TL, Lee JH, Park G, Pham DH, et al. Near-infrared illumination of native tissues for image-guided surgery. *J Med Chem* (2016) 59(11):5311–23. doi:10.1021/acs.jmedchem.6b00038
82. Stummer W, Stocker S, Wagner S, Stepp H, Fritsch C, Goetz C, et al. Intraoperative detection of malignant gliomas by 5-aminolevulinic acid-induced porphyrin fluorescence. *Neurosurgery* (1998) 42(3):518–25; discussion 525–6. doi:10.1097/00006123-199803000-00017
83. Stummer W, Pichlmeier U, Meinel T, Wiestler OD, Zanella F, Reulen HJ. Fluorescence-guided surgery with 5-aminolevulinic acid for resection of malignant glioma: a randomised controlled multicentre phase III trial. *Lancet Oncol* (2006) 7(5):392–401. doi:10.1016/s1470-2045(06)70665-9
84. Roberts DW, Valdes PA, Harris BT, Fontaine KM, Hartov A, Fan X, et al. Coregistered fluorescence-enhanced tumor resection of malignant glioma: relationships between delta-aminolevulinic acid-induced protoporphyrin IX fluorescence, magnetic resonance imaging enhancement, and neuropathological parameters. Clinical article. *J Neurosurg* (2011) 114(3):595–603. doi:10.3171/2010.2.jns091322
85. Colditz MJ, Jeffree RL. Aminolevulinic acid (ALA)-protoporphyrin IX fluorescence guided tumour resection. Part 1: clinical, radiological and pathological studies. *J Clin Neurosci* (2012) 19(11):1471–4. doi:10.1016/j.jocn.2012.03.009
86. Colditz MJ, Leyen K, Jeffree RL. Aminolevulinic acid (ALA)-protoporphyrin IX fluorescence guided tumour resection. Part 2: theoretical, biochemical and practical aspects. *J Clin Neurosci* (2012) 19(12):1611–6. doi:10.1016/j.jocn.2012.03.013
87. Kuroiwa T, Kajimoto Y, Ohta T. Development of a fluorescein operative microscope for use during malignant glioma surgery: a technical note and preliminary report. *Surg Neurol* (1998) 50(1):41–8; discussion 48–49. doi:10.1016/S0090-3019(98)00055-X
88. Shinoda J, Yano H, Yoshimura S, Okumura A, Kaku Y, Iwama T, et al. Fluorescence-guided resection of glioblastoma multiforme by using high-dose fluorescein sodium. Technical note. *J Neurosurg* (2003) 99(3):597–603. doi:10.3171/jns.2003.99.3.0597
89. Okuda T, Yoshioka H, Kato A. Fluorescence-guided surgery for glioblastoma multiforme using high-dose fluorescein sodium with excitation and barrier filters. *J Clin Neurosci* (2012) 19(12):1719–22. doi:10.1016/j.jocn.2011.12.034
90. Butte PV, Mamelak A, Parrish-Novak J, Drazin D, Shweikeh F, Gangalum PR, et al. Near-infrared imaging of brain tumors using the Tumor Paint BLZ-100 to achieve near-complete resection of brain tumors. *Neurosurg Focus* (2014) 36(2):E1. doi:10.3171/2013.11.focus13497
91. Cutter JL, Cohen NT, Wang J, Sloan AE, Cohen AR, Panneerselvam A, et al. Topical application of activity-based probes for visualization of brain tumor tissue. *PLoS One* (2012) 7(3):e33060. doi:10.1371/journal.pone.0033060
92. Okuda T, Kataoka K, Taneda M. Metastatic brain tumor surgery using fluorescein sodium: technical note. *Minim Invasive Neurosurg* (2007) 50(6):382–4. doi:10.1055/s-2007-993200
93. Okuda T, Kataoka K, Yabuuchi T, Yugami H, Kato A. Fluorescence-guided surgery of metastatic brain tumors using fluorescein sodium. *J Clin Neurosci* (2010) 17(1):118–21. doi:10.1016/j.jocn.2009.06.033
94. de Boer E, Warram JM, Tucker MD, Hartman YE, Moore LS, de Jong JS, et al. In vivo fluorescence immunohistochemistry: localization of fluorescently labeled cetuximab in squamous cell carcinomas. *Sci Rep* (2015) 5:10169. doi:10.1038/srep10169
95. Rosenthal EL, Warram JM, de Boer E, Chung TK, Korb ML, Brandwein-Gensler M, et al. Safety and tumor specificity of cetuximab-IRDye800 for surgical navigation in head and neck cancer. *Clin Cancer Res* (2015) 21(16):3658–66. doi:10.1158/1078-0432.ccr-14-3284
96. Mitsunaga M, Ogawa M, Kosaka N, Rosenblum LT, Choyke PL, Kobayashi H. Cancer cell-selective in vivo near infrared photoimmunotherapy targeting specific membrane molecules. *Nat Med* (2011) 17(12):1685–91. doi:10.1038/nm.2554
97. Cherrick GR, Stein SW, Leevy CM, Davidson CS. Indocyanine green: observations on its physical properties, plasma decay, and hepatic extraction. *J Clin Invest* (1960) 39:592–600. doi:10.1172/jci104072
98. Gotoh K, Yamada T, Ishikawa O, Takahashi H, Eguchi H, Yano M, et al. A novel image-guided surgery of hepatocellular carcinoma by indocyanine green fluorescence imaging navigation. *J Surg Oncol* (2009) 100(1):75–9. doi:10.1002/jso.21272
99. Ishizawa T, Fukushima N, Shibahara J, Masuda K, Tamura S, Aoki T, et al. Real-time identification of liver cancers by using indocyanine green fluorescent imaging. *Cancer* (2009) 115(11):2491–504. doi:10.1002/cncr.24291
100. Uchiyama K, Ueno M, Ozawa S, Kiriyama S, Shigekawa Y, Yamaue H. Combined use of contrast-enhanced intraoperative ultrasonography and a fluorescence navigation system for identifying hepatic metastases. *World J Surg* (2010) 34(12):2953–9. doi:10.1007/s00268-010-0764-1
101. Tummers QR, Verbeek FP, Schaafsma BE, Boonstra MC, van der Vorst JR, Liefers GJ, et al. Real-time intraoperative detection of breast cancer using

near-infrared fluorescence imaging and methylene blue. *Eur J Surg Oncol* (2014) 40(7):850–8. doi:10.1016/j.ejso.2014.02.225
102. Tipirneni KE, Warram JM, Moore LS, Prince AC, de Boer E, Jani AH, et al. Oncologic procedures amenable to fluorescence-guided surgery. *Ann Surg* (2017) 266(1):36–47. doi:10.1097/sla.0000000000002127
103. Whitley MJ, Cardona DM, Lazarides AL, Spasojevic I, Ferrer JM, Cahill J, et al. A mouse-human phase 1 co-clinical trial of a protease-activated fluorescent probe for imaging cancer. *Sci Transl Med* (2016) 8(320):320ra324. doi:10.1126/scitranslmed.aad0293
104. Unkart JT, Chen SL, Wapnir IL, Gonzalez JE, Harootunian A, Wallace AM. Intraoperative tumor detection using a ratiometric activatable fluorescent peptide: a first-in-human phase 1 study. *Ann Surg Oncol* (2017) 24(11): 3167–73. doi:10.1245/s10434-017-5991-3
105. Holt D, Okusanya O, Judy R, Venegas O, Jiang J, DeJesus E, et al. Intraoperative near-infrared imaging can distinguish cancer from normal tissue but not inflammation. *PLoS One* (2014) 9(7):e103342. doi:10.1371/journal.pone.0103342
106. Okusanya OT, DeJesus EM, Jiang JX, Judy RP, Venegas OG, Deshpande CG, et al. Intraoperative molecular imaging can identify lung adenocarcinomas during pulmonary resection. *J Thorac Cardiovasc Surg* (2015) 150(1):28–35. e1. doi:10.1016/j.jtcvs.2015.05.014
107. Predina JD, Okusanya O, D Newton A, Low P, Singhal S. Standardization and optimization of intraoperative molecular imaging for identifying primary pulmonary adenocarcinomas. *Mol Imaging Biol* (2017). doi:10.1007/s11307-017-1076-8
108. Predina JD, Newton AD, Keating J, Barbosa EM Jr, Okusanya O, Xia L, et al. Intraoperative molecular imaging combined with positron emission tomography improves surgical management of peripheral malignant pulmonary nodules. *Ann Surg* (2017) 266(3):479–88. doi:10.1097/sla.0000000000002382
109. Tummers QR, Hoogstins CE, Peters AA, de Kroon CD, Trimbos JB, van de Velde CJ, et al. The value of intraoperative near-infrared fluorescence imaging based on enhanced permeability and retention of indocyanine green: feasibility and false-positives in ovarian cancer. *PLoS One* (2015) 10(6):e0129766. doi:10.1371/journal.pone.0129766
110. Tummers QR, Hoogstins CE, Gaarenstroom KN, de Kroon CD, van Poelgeest MI, Vuyk J, et al. Intraoperative imaging of folate receptor alpha positive ovarian and breast cancer using the tumor specific agent EC17. *Oncotarget* (2016) 7(22):32144–55. doi:10.18632/oncotarget.8282
111. Hoogstins CE, Tummers QR, Gaarenstroom KN, de Kroon CD, Trimbos JB, Bosse T, et al. A novel tumor-specific agent for intraoperative near-infrared fluorescence imaging: a translational study in healthy volunteers and patients with ovarian cancer. *Clin Cancer Res* (2016) 22(12):2929–38. doi:10.1158/1078-0432.ccr-15-2640
112. Urano Y, Sakabe M, Kosaka N, Ogawa M, Mitsunaga M, Asanuma D, et al. Rapid cancer detection by topically spraying a gamma-glutamyltranspeptidase-activated fluorescent probe. *Sci Transl Med* (2011) 3 (110):110ra119. doi:10.1126/scitranslmed.3002823
113. Kaushal S, McElroy MK, Luiken GA, Talamini MA, Moossa AR, Hoffman RM, et al. Fluorophore-conjugated anti-CEA antibody for the intraoperative imaging of pancreatic and colorectal cancer. *J Gastrointest Surg* (2008) 12(11): 1938–50. doi:10.1007/s11605-008-0581-0
114. McElroy M, Kaushal S, Luiken GA, Talamini MA, Moossa AR, Hoffman RM, et al. Imaging of primary and metastatic pancreatic cancer using a fluorophore-conjugated anti-CA19-9 antibody for surgical navigation. *World J Surg* (2008) 32(6):1057–66. doi:10.1007/s00268-007-9452-1
115. van der Vorst JR, Vahrmeijer AL, Hutteman M, Bosse T, Smit VT, van de Velde CJ, et al. Near-infrared fluorescence imaging of a solitary fibrous tumor of the pancreas using methylene blue. *World J Gastrointest Surg* (2012) 4(7):180–4. doi:10.4240/wjgs.v4.i7.180
116. Guzzo TJ, Jiang J, Keating J, DeJesus E, Judy R, Nie S, et al. Intraoperative molecular diagnostic imaging can identify renal cell carcinoma. *J Urol* (2016) 195(3):748–55. doi:10.1016/j.juro.2015.09.093
117. Jichlinski P, Forrer M, Mizeret J, Glanzmann T, Braichotte D, Wagnieres G, et al. Clinical evaluation of a method for detecting superficial surgical transitional cell carcinoma of the bladder by light-induced fluorescence of protoporphyrin IX following the topical application of 5-aminolevulinic acid: preliminary results. *Lasers Surg Med* (1997) 20(4):402–8. doi:10.1002/(SICI)1096-9101(1997)20:4<402::AID-LSM5>3.0.CO;2-U
118. Jichlinski P, Guillou L, Karlsen SJ, Malmstrom PU, Jocham D, Brennhovd B, et al. Hexyl aminolevulinate fluorescence cystoscopy: new diagnostic tool for photodiagnosis of superficial bladder cancer – a multicenter study. *J Urol* (2003) 170(1):226–9. doi:10.1097/01.ju.0000060782.52358.04
119. Stenzl A, Burger M, Fradet Y, Mynderse LA, Soloway MS, Witjes JA, et al. Hexaminolevulinate guided fluorescence cystoscopy reduces recurrence in patients with nonmuscle invasive bladder cancer. *J Urol* (2010) 184(5):1907–13. doi:10.1016/j.juro.2010.06.148
120. Rink M, Babjuk M, Catto JW, Jichlinski P, Shariat SF, Stenzl A, et al. Hexyl aminolevulinate-guided fluorescence cystoscopy in the diagnosis and follow-up of patients with non-muscle-invasive bladder cancer: a critical review of the current literature. *Eur Urol* (2013) 64(4):624–38. doi:10.1016/j.eururo.2013.07.007
121. Nakajima T, Mitsunaga M, Bander NH, Heston WD, Choyke PL, Kobayashi H. Targeted, activatable, in vivo fluorescence imaging of prostate-specific membrane antigen (PSMA) positive tumors using the quenched humanized J591 antibody-indocyanine green (ICG) conjugate. *Bioconjug Chem* (2011) 22(8):1700–5. doi:10.1021/bc2002715
122. Fukuhara H, Inoue K, Kurabayashi A, Furihata M, Shuin T. Performance of 5-aminolevulinic-acid-based photodynamic diagnosis for radical prostatectomy. *BMC Urol* (2015) 15:78. doi:10.1186/s12894-015-0073-y
123. Iseki K, Tatsuta M, Iishi H, Sakai N, Yano H, Ishiguro S. Effectiveness of the near-infrared electronic endoscope for diagnosis of the depth of involvement of gastric cancers. *Gastrointest Endosc* (2000) 52(6):755–62. doi:10.1067/mge.2000.110455
124. Mataki N, Nagao S, Kawaguchi A, Matsuzaki K, Miyazaki J, Kitagawa Y, et al. Clinical usefulness of a new infrared videoendoscope system for diagnosis of early stage gastric cancer. *Gastrointest Endosc* (2003) 57(3): 336–42. doi:10.1067/mge.2003.133
125. Kimura T, Muguruma N, Ito S, Okamura S, Imoto Y, Miyamoto H, et al. Infrared fluorescence endoscopy for the diagnosis of superficial gastric tumors. *Gastrointest Endosc* (2007) 66(1):37–43. doi:10.1016/j.gie.2007.01.009
126. Gong L, Ding H, Long NE, Sullivan BJ, Martin EW Jr, Magliery TJ, et al. A 3E8.scFv.Cys-IR800 conjugate targeting TAG-72 in an orthotopic colorectal cancer model. *Mol Imaging Biol* (2017). doi:10.1007/s11307-017-1096-4
127. Mitsunaga M, Kosaka N, Choyke PL, Young MR, Dextras CR, Saud SM, et al. Fluorescence endoscopic detection of murine colitis-associated colon cancer by topically applied enzymatically rapid-activatable probe. *Gut* (2013) 62(8):1179–86. doi:10.1136/gutjnl-2011-301795
128. Alkalay R, Alcalay J, Maly A, Ingber A, Fritsch C, Ruzicka T, et al. Fluorescence imaging for the demarcation of basal cell carcinoma tumor borders. *J Drugs Dermatol* (2008) 7(11):1033–7.
129. Walker E, Mann M, Honda K, Vidimos A, Schluchter MD, Straight B, et al. Rapid visualization of nonmelanoma skin cancer. *J Am Acad Dermatol* (2017) 76(2): 209–216.e9. doi:10.1016/j.jaad.2016.09.008
130. van der Vorst JR, Schaafsma BE, Verbeek FP, Swijnenburg RJ, Tummers QR, Hutteman M, et al. Intraoperative near-infrared fluorescence imaging of parathyroid adenomas with use of low-dose methylene blue. *Head Neck* (2014) 36(6):853–8. doi:10.1002/hed.23384
131. Tobis S, Knopf J, Silvers C, Yao J, Rashid H, Wu G, et al. Near infrared fluorescence imaging with robotic assisted laparoscopic partial nephrectomy: initial clinical experience for renal cortical tumors. *J Urol* (2011) 186(1):47–52. doi:10.1016/j.juro.2011.02.2701
132. Morita K, Ishizawa T, Tani K, Harada N, Shimizu A, Yamamoto S, et al. Application of indocyanine green-fluorescence imaging to full-thickness cholecystectomy. *Asian J Endosc Surg* (2014) 7(2):193–5. doi:10.1111/ases.12083
133. Schlottmann F, Patti MG. Evaluation of gastric conduit perfusion during esophagectomy with indocyanine green fluorescence imaging. *J Laparoendosc Adv Surg Tech A* (2017) 27(12):1305–8. doi:10.1089/lap.2017.0359
134. Kim M, Son SY. Real-time vessel navigation using indocyanine green fluorescence during robotic or laparoscopic gastrectomy for gastric cancer. *J Gastric Cancer* (2017) 17(2):145–53. doi:10.5230/jgc.2017.17.e17
135. Manny TB, Pompeo AS, Hemal AK. Robotic partial adrenalectomy using indocyanine green dye with near-infrared imaging: the initial clinical experience. *Urology* (2013) 82(3):738–42. doi:10.1016/j.urology.2013.03.074

136. Colvin J, Zaidi N, Berber E. The utility of indocyanine green fluorescence imaging during robotic adrenalectomy. *J Surg Oncol* (2016) 114(2):153–6. doi:10.1002/jso.24296
137. Nishiyama Y, Kinouchi H, Senbokuya N, Kato T, Kanemaru K, Yoshioka H, et al. Endoscopic indocyanine green video angiography in aneurysm surgery: an innovative method for intraoperative assessment of blood flow in vasculature hidden from microscopic view. *J Neurosurg* (2012) 117(2):302–8. doi:10.3171/2012.5.jns112300
138. Bruneau M, Appelboom G, Rynkowski M, Van Cutsem N, Mine B, De Witte O. Endoscope-integrated ICG technology: first application during intracranial aneurysm surgery. *Neurosurg Rev* (2013) 36(1):77–84; discussion 84–5. doi:10.1007/s10143-012-0419-9
139. Mielke D, Malinova V, Rohde V. Comparison of intraoperative microscopic and endoscopic ICG angiography in aneurysm surgery. *Neurosurgery* (2014) 10(Suppl 3):418–25; discussion 425. doi:10.1227/neu.0000000000000345
140. Litvack ZN, Zada G, Laws ER Jr. Indocyanine green fluorescence endoscopy for visual differentiation of pituitary tumor from surrounding structures. *J Neurosurg* (2012) 116(5):935–41. doi:10.3171/2012.1.jns11601
141. Hide T, Yano S, Shinojima N, Kuratsu J. Usefulness of the indocyanine green fluorescence endoscope in endonasal transsphenoidal surgery. *J Neurosurg* (2015) 122(5):1185–92. doi:10.3171/2014.9.jns14599
142. Simal Julian JA, Sanroman Alvarez P, Miranda Lloret P, Botella Asuncion C. Endo ICG videoangiography: localizing the carotid artery in skull-base endonasal approaches. *Acta Neurochir (Wien)* (2016) 158(7):1351–3. doi:10.1007/s00701-016-2830-4
143. Wachter D, Behm T, von Eckardstein K, Rohde V. Indocyanine green angiography in endoscopic third ventriculostomy. *Neurosurgery* (2013) 73 (1 Suppl Operative):ons67–72. doi:10.1227/NEU.0b013e318285b846
144. Foersch S, Heimann A, Ayyad A, Spoden GA, Florin L, Mpoukouvalas K, et al. Confocal laser endomicroscopy for diagnosis and histomorphologic imaging of brain tumors in vivo. *PLoS One* (2012) 7(7):e41760. doi:10.1371/journal.pone.0041760
145. Tsuzuki S, Aihara Y, Eguchi S, Amano K, Kawamata T, Okada Y. Application of indocyanine green (ICG) fluorescence for endoscopic biopsy of intraventricular tumors. *Childs Nerv Syst* (2014) 30(4):723–6. doi:10.1007/s00381-013-2266-6
146. Schmidt F, Dittberner A, Koscielny S, Petersen I, Guntinas-Lichius O. Feasibility of real-time near-infrared indocyanine green fluorescence endoscopy for the evaluation of mucosal head and neck lesions. *Head Neck* (2017) 39(2):234–40. doi:10.1002/hed.24570
147. Lee JG, Low AH, Leung JW. Randomized comparative study of indocyanine green and India ink for colonic tattooing: an animal survival study. *J Clin Gastroenterol* (2000) 31(3):233–6. doi:10.1097/00004836-200010000-00010
148. Miyoshi N, Ohue M, Noura S, Yano M, Sasaki Y, Kishi K, et al. Surgical usefulness of indocyanine green as an alternative to India ink for endoscopic marking. *Surg Endosc* (2009) 23(2):347–51. doi:10.1007/s00464-008-9938-4
149. Watanabe M, Tsunoda A, Narita K, Kusano M, Miwa M. Colonic tattooing using fluorescence imaging with light-emitting diode-activated indocyanine green: a feasibility study. *Surg Today* (2009) 39(3):214–8. doi:10.1007/s00595-008-3849-9
150. Gray D, Kim E, Cotero V, Staudinger P, Yazdanfar S, Hehir CT. Compact fluorescence and white light imaging system for intraoperative visualization of nerves. *Proc SPIE Int Soc Opt Eng* (2012) 8207. doi:10.1117/12.905354
151. Keereweer S, Mol IM, Vahrmeijer AL, Van Driel PB, Baatenburg de Jong RJ, Kerrebijn JD, et al. Dual wavelength tumor targeting for detection of hypopharyngeal cancer using near-infrared optical imaging in an animal model. *Int J Cancer* (2012) 131(7):1633–40. doi:10.1002/ijc.27430
152. Wapnir I, Dua M, Kieryn A, Paro J, Morrison D, Kahn D, et al. Intraoperative imaging of nipple perfusion patterns and ischemic complications in nipple-sparing mastectomies. *Ann Surg Oncol* (2014) 21(1):100–6. doi:10.1245/s10434-013-3214-0
153. Richards-Kortum R, Sevick-Muraca E. Quantitative optical spectroscopy for tissue diagnosis. *Annu Rev Phys Chem* (1996) 47:555–606. doi:10.1146/annurev.physchem.47.1.555
154. Hilderbrand SA, Weissleder R. Near-infrared fluorescence: application to in vivo molecular imaging. *Curr Opin Chem Biol* (2010) 14(1):71–9. doi:10.1016/j.cbpa.2009.09.029
155. Kobayashi H, Ogawa M, Alford R, Choyke PL, Urano Y. New strategies for fluorescent probe design in medical diagnostic imaging. *Chem Rev* (2010) 110(5):2620–40. doi:10.1021/cr900263j
156. Chance B. Near-infrared images using continuous, phase-modulated, and pulsed light with quantitation of blood and blood oxygenation. *Ann N Y Acad Sci* (1998) 838:29–45. doi:10.1111/j.1749-6632.1998.tb08185.x
157. Bouvet M, Hoffman RM. Glowing tumors make for better detection and resection. *Sci Transl Med* (2011) 3(110):110fs110. doi:10.1126/scitranslmed.3003375
158. Moody ED, Viskari PJ, Colyer CL. Non-covalent labeling of human serum albumin with indocyanine green: a study by capillary electrophoresis with diode laser-induced fluorescence detection. *J Chromatogr B Biomed Sci Appl* (1999) 729(1–2):55–64. doi:10.1016/S0378-4347(99)00121-8
159. Ogawa M, Kosaka N, Choyke PL, Kobayashi H. In vivo molecular imaging of cancer with a quenching near-infrared fluorescent probe using conjugates of monoclonal antibodies and indocyanine green. *Cancer Res* (2009) 69(4):1268–72. doi:10.1158/0008-5472.can-08-3116
160. Tanaka E, Chen FY, Flaumenhaft R, Graham GJ, Laurence RG, Frangioni JV. Real-time assessment of cardiac perfusion, coronary angiography, and acute intravascular thrombi using dual-channel near-infrared fluorescence imaging. *J Thorac Cardiovasc Surg* (2009) 138(1):133–40. doi:10.1016/j.jtcvs.2008.09.082
161. Deja M, Ahlers O, Macguill M, Wust P, Hildebrandt B, Riess H, et al. Changes in hepatic blood flow during whole body hyperthermia. *Int J Hyperthermia* (2010) 26(2):95–100. doi:10.3109/02656730903250574
162. Kang SW, Chung SE, Shin WJ, Lee JH. Polypoidal choroidal vasculopathy and late geographic hyperfluorescence on indocyanine green angiography. *Br J Ophthalmol* (2009) 93(6):759–64. doi:10.1136/bjo.2008.145862
163. Alford R, Simpson HM, Duberman J, Hill GC, Ogawa M, Regino C, et al. Toxicity of organic fluorophores used in molecular imaging: literature review. *Mol Imaging* (2009) 8(6):341–54. doi:10.2310/7290.2009.00031
164. Kudszus S, Roesel C, Schachtrupp A, Hoer JJ. Intraoperative laser fluorescence angiography in colorectal surgery: a noninvasive analysis to reduce the rate of anastomotic leakage. *Langenbecks Arch Surg* (2010) 395(8):1025–30. doi:10.1007/s00423-010-0699-x
165. Schaafsma BE, Mieog JS, Hutteman M, van der Vorst JR, Kuppen PJ, Lowik CW, et al. The clinical use of indocyanine green as a near-infrared fluorescent contrast agent for image-guided oncologic surgery. *J Surg Oncol* (2011) 104(3):323–32. doi:10.1002/jso.21943
166. Shimizu S, Kamiike W, Hatanaka N, Yoshida Y, Tagawa K, Miyata M, et al. New method for measuring ICG Rmax with a clearance meter. *World J Surg* (1995) 19(1):113–8; discussion 118. doi:10.1007/BF00316992
167. Kung TA, Champaneria MC, Maki JH, Neligan PC. Current concepts in the surgical management of lymphedema. *Plast Reconstr Surg* (2017) 139(4):1003e–13e. doi:10.1097/prs.0000000000003218
168. Champagne BJ, Darling RC III, Daneshmand M, Kreienberg PB, Lee EC, Mehta M, et al. Outcome of aggressive surveillance colonoscopy in ruptured abdominal aortic aneurysm. *J Vasc Surg* (2004) 39(4):792–6. doi:10.1016/j.jvs.2003.12.002
169. Schirmer RH, Adler H, Pickhardt M, Mandelkow E. Lest we forget you – methylene blue…. *Neurobiol Aging* (2011) 32(12): 2325.e7–16. doi:10.1016/j.neurobiolaging.2010.12.012
170. Ashurst J, Wasson M. Methemoglobinemia: a systematic review of the pathophysiology, detection, and treatment. *Del Med J* (2011) 83(7):203–8.
171. Richards A, Marshall H, McQuary A. Evaluation of methylene blue, thiamine, and/or albumin in the prevention of ifosfamide-related neurotoxicity. *J Oncol Pharm Pract* (2011) 17(4):372–80. doi:10.1177/1078155210385159
172. Ginimuge PR, Jyothi SD. Methylene blue: revisited. *J Anaesthesiol Clin Pharmacol* (2010) 26(4):517–20.
173. Melo TB, Reisaeter G. The physicochemical state of protoporphyrin IX in aqueous solution investigated by fluorescence and light scattering. *Biophys Chem* (1986) 25(1):99–104. doi:10.1016/0301-4622(86)85070-0
174. Montcel B, Mahieu-Williame L, Armoiry X, Meyronet D, Guyotat J. Two-peaked 5-ALA-induced PpIX fluorescence emission spectrum distinguishes glioblastomas from low grade gliomas and infiltrative component of glioblastomas. *Biomed Opt Express* (2013) 4(4):548–58. doi:10.1364/boe.4.000548
175. Acerbi F, Broggi M, Eoli M, Anghileri E, Cuppini L, Pollo B, et al. Fluorescein-guided surgery for grade IV gliomas with a dedicated filter on the surgical

microscope: preliminary results in 12 cases. *Acta Neurochir (Wien)* (2013) 155(7):1277–86. doi:10.1007/s00701-013-1734-9
176. Acerbi F, Broggi M, Eoli M, Anghileri E, Cavallo C, Boffano C, et al. Is fluorescein-guided technique able to help in resection of high-grade gliomas? *Neurosurg Focus* (2014) 36(2):E5. doi:10.3171/2013.11.focus13487
177. Diaz RJ, Dios RR, Hattab EM, Burrell K, Rakopoulos P, Sabha N, et al. Study of the biodistribution of fluorescein in glioma-infiltrated mouse brain and histopathological correlation of intraoperative findings in high-grade gliomas resected under fluorescein fluorescence guidance. *J Neurosurg* (2015) 122(6):1360–9. doi:10.3171/2015.2.jns132507
178. Schwake M, Stummer W, Suero Molina EJ, Wolfer J. Simultaneous fluorescein sodium and 5-ALA in fluorescence-guided glioma surgery. *Acta Neurochir (Wien)* (2015) 157(5):877–9. doi:10.1007/s00701-015-2401-0
179. Moore GE. Fluorescein as an agent in the differentiation of normal and malignant tissues. *Science* (1947) 106(2745):130–1. doi:10.1126/science.106.2745.130-a
180. Te Velde EA, Veerman T, Subramaniam V, Ruers T. The use of fluorescent dyes and probes in surgical oncology. *Eur J Surg Oncol* (2010) 36(1):6–15. doi:10.1016/j.ejso.2009.10.014
181. Gioux S, Choi HS, Frangioni JV. Image-guided surgery using invisible near-infrared light: fundamentals of clinical translation. *Mol Imaging* (2010) 9(5):237–55.
182. Terwisscha van Scheltinga AG, van Dam GM, Nagengast WB, Ntziachristos V, Hollema H, Herek JL, et al. Intraoperative near-infrared fluorescence tumor imaging with vascular endothelial growth factor and human epidermal growth factor receptor 2 targeting antibodies. *J Nucl Med* (2011) 52(11):1778–85. doi:10.2967/jnumed.111.092833
183. Sano K, Mitsunaga M, Nakajima T, Choyke PL, Kobayashi H. In vivo breast cancer characterization imaging using two monoclonal antibodies activatably labeled with near infrared fluorophores. *Breast Cancer Res* (2012) 14(2):R61. doi:10.1186/bcr3167
184. Oliveira S, van Dongen GA, Stigter-van Walsum M, Roovers RC, Stam JC, Mali W, et al. Rapid visualization of human tumor xenografts through optical imaging with a near-infrared fluorescent anti-epidermal growth factor receptor nanobody. *Mol Imaging* (2012) 11(1):33–46. doi:10.2310/7290.2011.00025
185. Blum G, von Degenfeld G, Merchant MJ, Blau HM, Bogyo M. Noninvasive optical imaging of cysteine protease activity using fluorescently quenched activity-based probes. *Nat Chem Biol* (2007) 3(10):668–77. doi:10.1038/nchembio.2007.26
186. Blum G, Weimer RM, Edgington LE, Adams W, Bogyo M. Comparative assessment of substrates and activity based probes as tools for non-invasive optical imaging of cysteine protease activity. *PLoS One* (2009) 4(7):e6374. doi:10.1371/journal.pone.0006374
187. Olson ES, Jiang T, Aguilera TA, Nguyen QT, Ellies LG, Scadeng M, et al. Activatable cell penetrating peptides linked to nanoparticles as dual probes for in vivo fluorescence and MR imaging of proteases. *Proc Natl Acad Sci U S A* (2010) 107(9):4311–6. doi:10.1073/pnas.0910283107
188. Deu E, Verdoes M, Bogyo M. New approaches for dissecting protease functions to improve probe development and drug discovery. *Nat Struct Mol Biol* (2012) 19(1):9–16. doi:10.1038/nsmb.2203
189. Olson ES, Whitney MA, Friedman B, Aguilera TA, Crisp JL, Baik FM, et al. In vivo fluorescence imaging of atherosclerotic plaques with activatable cell-penetrating peptides targeting thrombin activity. *Integr Biol (Camb)* (2012) 4(6):595–605. doi:10.1039/c2ib00161f
190. Lu Y, Low PS. Folate targeting of haptens to cancer cell surfaces mediates immunotherapy of syngeneic murine tumors. *Cancer Immunol Immunother* (2002) 51(3):153–62. doi:10.1007/s00262-002-0266-6
191. Leamon CP, Low PS. Delivery of macromolecules into living cells: a method that exploits folate receptor endocytosis. *Proc Natl Acad Sci U S A* (1991) 88(13):5572–6. doi:10.1073/pnas.88.13.5572
192. Low PS, Henne WA, Doorneweerd DD. Discovery and development of folic-acid-based receptor targeting for imaging and therapy of cancer and inflammatory diseases. *Acc Chem Res* (2008) 41(1):120–9. doi:10.1021/ar7000815
193. Weitman SD, Lark RH, Coney LR, Fort DW, Frasca V, Zurawski VR Jr, et al. Distribution of the folate receptor GP38 in normal and malignant cell lines and tissues. *Cancer Res* (1992) 52(12):3396–401.
194. O'Shannessy DJ, Yu G, Smale R, Fu YS, Singhal S, Thiel RP, et al. Folate receptor alpha expression in lung cancer: diagnostic and prognostic significance. *Oncotarget* (2012) 3(4):414–25. doi:10.18632/oncotarget.489
195. Ogawa M, Kosaka N, Choyke PL, Kobayashi H. H-type dimer formation of fluorophores: a mechanism for activatable, in vivo optical molecular imaging. *ACS Chem Biol* (2009) 4(7):535–46. doi:10.1021/cb900089j
196. Ogawa M, Kosaka N, Longmire MR, Urano Y, Choyke PL, Kobayashi H. Fluorophore-quencher based activatable targeted optical probes for detecting in vivo cancer metastases. *Mol Pharm* (2009) 6(2):386–95. doi:10.1021/mp800115t
197. Ogawa M, Regino CA, Choyke PL, Kobayashi H. In vivo target-specific activatable near-infrared optical labeling of humanized monoclonal antibodies. *Mol Cancer Ther* (2009) 8(1):232–9. doi:10.1158/1535-7163.mct-08-0862
198. Hanaoka H, Nagaya T, Sato K, Nakamura Y, Watanabe R, Harada T, et al. Glypican-3 targeted human heavy chain antibody as a drug carrier for hepatocellular carcinoma therapy. *Mol Pharm* (2015) 12(6):2151–7. doi:10.1021/acs.molpharmaceut.5b00132
199. Sato K, Nagaya T, Choyke PL, Kobayashi H. Near infrared photoimmunotherapy in the treatment of pleural disseminated NSCLC: preclinical experience. *Theranostics* (2015) 5(7):698–709. doi:10.7150/thno.11559
200. Nagaya T, Nakamura Y, Sato K, Harada T, Choyke PL, Kobayashi H. Near infrared photoimmunotherapy of B-cell lymphoma. *Mol Oncol* (2016) 10(9):1404–14. doi:10.1016/j.molonc.2016.07.010
201. Nagaya T, Nakamura Y, Sato K, Zhang YF, Ni M, Choyke PL, et al. Near infrared photoimmunotherapy with an anti-mesothelin antibody. *Oncotarget* (2016) 7(17):23361–9. doi:10.18632/oncotarget.8025
202. Nagaya T, Nakamura Y, Okuyama S, Ogata F, Maruoka Y, Choyke PL, et al. Near-infrared photoimmunotherapy targeting prostate cancer with prostate-specific membrane antigen (PSMA) antibody. *Mol Cancer Res* (2017) 15(9):1153–62. doi:10.1158/1541-7786.mcr-17-0164
203. Kobayashi H, Choyke PL. Target-cancer-cell-specific activatable fluorescence imaging probes: rational design and in vivo applications. *Acc Chem Res* (2011) 44(2):83–90. doi:10.1021/ar1000633
204. Chi C, Zhang Q, Mao Y, Kou D, Qiu J, Ye J, et al. Increased precision of orthotopic and metastatic breast cancer surgery guided by matrix metalloproteinase-activatable near-infrared fluorescence probes. *Sci Rep* (2015) 5:14197. doi:10.1038/srep14197
205. Weissleder R. A clearer vision for in vivo imaging. *Nat Biotechnol* (2001) 19(4):316–7. doi:10.1038/86684
206. Sheth RA, Upadhyay R, Stangenberg L, Sheth R, Weissleder R, Mahmood U. Improved detection of ovarian cancer metastases by intraoperative quantitative fluorescence protease imaging in a pre-clinical model. *Gynecol Oncol* (2009) 112(3):616–22. doi:10.1016/j.ygyno.2008.11.018
207. Urano Y, Asanuma D, Hama Y, Koyama Y, Barrett T, Kamiya M, et al. Selective molecular imaging of viable cancer cells with pH-activatable fluorescence probes. *Nat Med* (2009) 15(1):104–9. doi:10.1038/nm.1854
208. Mieog JS, Hutteman M, van der Vorst JR, Kuppen PJ, Que I, Dijkstra J, et al. Image-guided tumor resection using real-time near-infrared fluorescence in a syngeneic rat model of primary breast cancer. *Breast Cancer Res Treat* (2011) 128(3):679–89. doi:10.1007/s10549-010-1130-6
209. Ogawa M, Regino CA, Seidel J, Green MV, Xi W, Williams M, et al. Dual-modality molecular imaging using antibodies labeled with activatable fluorescence and a radionuclide for specific and quantitative targeted cancer detection. *Bioconjug Chem* (2009) 20(11):2177–84. doi:10.1021/bc900362k
210. Kobayashi H, Choyke PL, Ogawa M. Monoclonal antibody-based optical molecular imaging probes; considerations and caveats in chemistry, biology and pharmacology. *Curr Opin Chem Biol* (2016) 33:32–8. doi:10.1016/j.cbpa.2016.05.015
211. Hama Y, Urano Y, Koyama Y, Kamiya M, Bernardo M, Paik RS, et al. A target cell-specific activatable fluorescence probe for in vivo molecular imaging of cancer based on a self-quenched avidin-rhodamine conjugate. *Cancer Res* (2007) 67(6):2791–9. doi:10.1158/0008-5472.can-06-3315
212. Mahmood U, Tung CH, Bogdanov A Jr, Weissleder R. Near-infrared optical imaging of protease activity for tumor detection. *Radiology* (1999) 213(3):866–70. doi:10.1148/radiology.213.3.r99dc14866
213. Tung CH, Bredow S, Mahmood U, Weissleder R. Preparation of a cathepsin D sensitive near-infrared fluorescence probe for imaging. *Bioconjug Chem* (1999) 10(5):892–6. doi:10.1021/bc990052h

214. Urano Y. Novel live imaging techniques of cellular functions and in vivo tumors based on precise design of small molecule-based 'activatable' fluorescence probes. *Curr Opin Chem Biol* (2012) 16(5–6):602–8. doi:10.1016/j.cbpa.2012.10.023
215. Lotan R, Raz A. Lectins in cancer cells. *Ann N Y Acad Sci* (1988) 551:385–96; discussion 396–8. doi:10.1111/j.1749-6632.1988.tb22372.x
216. Ang CY, Tan SY, Lu Y, Bai L, Li M, Li P, et al. "Turn-on" fluorescence probe integrated polymer nanoparticles for sensing biological thiol molecules. *Sci Rep* (2014) 4:7057. doi:10.1038/srep07057
217. Shimizu Y, Temma T, Hara I, Makino A, Yamahara R, Ozeki E, et al. Micelle-based activatable probe for in vivo near-infrared optical imaging of cancer biomolecules. *Nanomedicine* (2014) 10(1):187–95. doi:10.1016/j.nano.2013.06.009
218. Feng T, Ai X, Ong H, Zhao Y. Dual-responsive carbon dots for tumor extracellular microenvironment triggered targeting and enhanced anticancer drug delivery. *ACS Appl Mater Interfaces* (2016) 8(29):18732–40. doi:10.1021/acsami.6b06695
219. Johansson MK, Cook RM. Intramolecular dimers: a new design strategy for fluorescence-quenched probes. *Chemistry* (2003) 9(15):3466–71. doi:10.1002/chem.200304941
220. Urano Y, Kamiya M, Kanda K, Ueno T, Hirose K, Nagano T. Evolution of fluorescein as a platform for finely tunable fluorescence probes. *J Am Chem Soc* (2005) 127(13):4888–94. doi:10.1021/ja043919h
221. Mohamed MM, Sloane BF. Cysteine cathepsins: multifunctional enzymes in cancer. *Nat Rev Cancer* (2006) 6(10):764–75. doi:10.1038/nrc1949
222. Tung CH, Mahmood U, Bredow S, Weissleder R. In vivo imaging of proteolytic enzyme activity using a novel molecular reporter. *Cancer Res* (2000) 60(17):4953–8.
223. Chen J, Tung CH, Allport JR, Chen S, Weissleder R, Huang PL. Near-infrared fluorescent imaging of matrix metalloproteinase activity after myocardial infarction. *Circulation* (2005) 111(14):1800–5. doi:10.1161/01.cir.0000160936.91849.9f
224. Sato C, Abe S, Saito Y, So Tsuruki E, Takamaru H, Makazu M, et al. A pilot study of fluorescent imaging of colorectal tumors using a gamma-glutamyl-transpeptidase-activatable fluorescent probe. *Digestion* (2015) 91(1):70–6. doi:10.1159/000369367
225. Ueo H, Shinden Y, Tobo T, Gamachi A, Udo M, Komatsu H, et al. Rapid intraoperative visualization of breast lesions with gamma-glutamyl hydroxymethyl rhodamine green. *Sci Rep* (2015) 5:12080. doi:10.1038/srep12080
226. Kawakubo K, Ohnishi S, Hatanaka Y, Hatanaka KC, Hosono H, Kubota Y, et al. Feasibility of using an enzymatically activatable fluorescence probe for the rapid evaluation of pancreatic tissue obtained using endoscopic ultrasound-guided fine needle aspiration: a pilot study. *Mol Imaging Biol* (2016) 18(3):463–71. doi:10.1007/s11307-015-0898-5
227. Asanuma D, Sakabe M, Kamiya M, Yamamoto K, Hiratake J, Ogawa M, et al. Sensitive beta-galactosidase-targeting fluorescence probe for visualizing small peritoneal metastatic tumours in vivo. *Nat Commun* (2015) 6:6463. doi:10.1038/ncomms7463
228. Sakabe M, Asanuma D, Kamiya M, Iwatate RJ, Hanaoka K, Terai T, et al. Rational design of highly sensitive fluorescence probes for protease and glycosidase based on precisely controlled spirocyclization. *J Am Chem Soc* (2013) 135(1):409–14. doi:10.1021/ja309688m
229. Shen Z, Prasai B, Nakamura Y, Kobayashi H, Jackson MS, McCarley RL. A near-infrared, wavelength-shiftable, turn-on fluorescent probe for the detection and imaging of cancer tumor cells. *ACS Chem Biol* (2017) 12(4):1121–32. doi:10.1021/acschembio.6b01094

Conflict of Interest Statement: The authors declare that the research was conducted in the absence of any commercial or financial relationships that could be construed as a potential conflict of interest.